Weak interaction studied in a few electron atomic ions

Katarzyna Siegien-Iwaniuk

Section of Theoretical Physics (N8)

National Centre for Nuclear Research

A thesis submitted for the degree of

Doctor of Physics

2012

I would like to dedicate this thesis to Maks.

Acknowledgements

Several people contributed significantly toward the completion of this thesis. The most, I am deeply grateful to Zygmunt Patyk, my research adviser, for providing me with opportunity to do low- energy theory during these past three years. His patient teaching, steady encouragement, and warm support have made this a valuable enriching experience. I am also grateful to my husband and my parents for their assistance and support during preparation of this thesis.

Abstract

In this thesis examples of the weak interactions in hydrogen-, helium- and lithium-like ions has been investigated theoretically. After a short historical introduction, the ratio of the probabilities of the orbital electron capture decay (EC) between H- and He-like ions as well as H- and Li-like ions are calculated. Corrections to the ratio of EC rates in hydrogen- and helium-like ions are also calculated. EC in helium-like ions with the emission of the un-captured electron in a new decay channel has been discussed. Using the sudden approximation, the ionisation probability of the $^6Li^{2+}$ daughter ions resulting from the β^- decay of $^6He^+$ ions has been calculated. In last chapter there is a short discussion of the weak neutral current (parity non-conservation effect). The thesis includes a brief discussion of experiments verifying and the possibilities of experimental verification of the analyzed predictions.

Streszczenie

W pracy została przeprowadzona teoretyczna analiza przykadłów oddziaływań słabych w jonach wodoro-, helo- i lito-podobnych. Po krótkim wstępie teoretycznym, zostały znalezione i zanalizowane zależności pomiędzy prawdopodobieństwami dla rozpadu poprzez wychwyt elektronowy (EC) dla jonów H- i He-podobnych oraz H- i Li-podobnych. Zostały policzone poprawki do tychże zależności w jonach wodoro- oraz helo-podobnych. Przedyskutowano EC w jonach helo-podobnych z emisją niewychwyconego elektronu jako nowy kanał rozpadu. Przy pomocy "sudden approximation", zostało znalezione prawdopodobieństwo jonizacji dla jonów $^6Li^{2+}$ powstałych w wyniku rozpadu β^- jonów $^6He^+$. W ostatniej części została przeprowadzona krótka dyskusja oddziaływań słabych prądów neutralnych. Rozprawa zawiera również krótką dyskusję eksperymentow przeprowadzonych oraz możliwych do przeprowadzenia weryfikujących analizowane w niniejszej pracy rozważania.

Contents

Introduction

The nuclear electron capture process in neutral atoms has been studied both theoretically and experimentally for many years. However, due to the large progress in the production, accumulation and diagnostics of radioactive beams, investigations of electron capture and beta-decay in highly charged ions have quite recently become possible.

For example, such experiments are performed at GSI Darmstadt, where single ions practically for any nucleus and in any charge state can be produced, separated and injected into the storage ring ESR. In a highly charged ion some new decay channels open that are not present in neutral atoms e.g. beta decay of the bare nucleus with electron emission to a bound state. Contrarily some decay modes known in neutral atoms can be forbidden in highly charged ions e.g. electron capture is disabled in the bare nucleus.

A few years ago GSI-Darmstadt started pioneering measurements of half-lives for single, highly charged H-like and He-like ions decaying by electron capture. The ratio of electron capture probabilities for H- and He-like ^{140}Pr ions was measured for the first time, yielding a result approximately equal to 3/2 that was completely unexpected [28, 44].

In the standard theory of the electron capture process, for a not completely filled 1s electron shell-as in the case of H-like and He-like ions-the electron capture probability is approximately proportional to the number of electrons. Therefore, the above mentioned ratio should be around 1/2 instead of the measured value of 3/2.

The first rough explanation of this puzzle was given in [52], assuming conservation of the total orbital momentum for H- and He-like ions and the electron density at the nucleus proportional to the number of electrons in the 1s shell.

However, the assumption that the interaction between electrons in a He-like ion can be neglected is not valid, especially for light nuclei e.g. for a parent nucleus ^{7}Be decaying by electron capture and discussed in the thesis.

In two papers, published in the Physical Review C [61, 62] a full and original explanation of this puzzle has been presented. The method applied is more general than that used in the previous paper [52]. In these papers the relation between electron capture probabilities for H-like, He-like and Li-like ions has been derived and is discussed in detail. Original results obtained in the papers are included in the thesis.

In the thesis a new decay channel for a He-like ion has been proposed; electron capture with simultaneous emission of the second electron into the continuum. The ionization probability has been calculated in the sudden approximation limit. However, this approximation has never been verified experimentally in atomic or nuclear physics.

Together with researchers from GANIL the sudden approximation has been tested in the beta decay of $^{6}He^{+}$. The measured $^{6}He^{+}$ ionization probability and that calculated in the sudden approximation limit are in perfect agreement. The original experimental and theoretical textbook results of the ionization probability have been published in Physical Review Letters [9] and are also discussed in detail in the thesis. Paper has been featured:
http://physics.aps.org/synopsis-for/10.1103/PhysRevLett.108.243201

Chapter 1

The scope of the weak interaction

The weak interaction is responsible for radioactive decays. In this chapter a short history of the weak interaction is presented, from Fermi's theory to parity non-conservation effects.

1.1 Short history of beta decay

The history of radioactivity began in 1896 with the discoveries of Henri Becquerel [5]. A few years later he identified beta radiation as one component of radioactivity, and demonstrated that beta rays are composed of electrons. But the real history of the controversies around beta decay starts about 1911, from the experiment of Lise Meitner and Otto Hahn, which showed that the energies of electrons emitted in beta decay had a continuous rather than discrete spectrum. This suggested energy non-conservation, but apparently not only was energy not conserved, but neither were momentum and angular momentum. This caused a great deal of anxiety among physicists around the world. In well known alpha and gamma decay, the emitted spectra were discrete simply because of energy conservation (the energy of the emitted particle and the recoil energy of the daughter nucleus are the same as the energy difference between the initial and final state of the nucleus). The observation that the energy of the emitted electrons in beta decay could take any value between zero and some certain maximum value was so bizarre that many more experiments followed. In fact Meitner and Hahn argued

that what they saw a was discrete spectrum, and it may only look like continuous because of energy loss in the material. Lack of consent and controversy lasted over a decade until 1927, when Ellis and Woosley dispelled all doubts in a very simple experiment. They measured the total energy released in the disintegration of a ^{210}Bi source inside a calorimeter thick enough to stop all the emitted electrons. The endpoint was known to be $E_0 = 1.05$ MeV, and the mean energy (E) of the electrons was known to be 390 keV. The calorimeter should have measured a total energy of 1.05 MeV if the above picture was correct. In fact they observed $E = 344 \pm 34$ keV, which corresponded very well with the mean energy of the emitted electrons. The spectrum was indeed continuous. This fact inspired even Niels Bohr, who said:

At the present stage of atomic theory, however, we may say that we have no argument, either empirical or theoretical, for upholding the energy principle in the case of beta-ray disintegration.

The first solution of the problem was given at last by Pauli in 1930. He suggested that in addition to electrons and protons in atoms, the existence of an extremely light neutral particle which he called the neutron. He also inspired the idea that this new particle was also emitted during beta decay and had simply not yet been observed. After the discovery of the real neutron by Chadwick in 1931, Enrico Fermi renamed Pauli's neutron the electron neutrino, and in 1934 published a very successful model of beta decay in which neutrinos were produced. He described the weak interaction by considering the Hamiltonian as the scalar product of two four-vectors. The Hamiltonian then becomes the scalar product of a hadronic vector current and a leptonic vector current [16]. Later, when Gamow-Teller transitions and parity non conservation were discovered, there were introduced corrections to Fermi's universal theory.

1.2 Review of beta decay

In the β decay process [4] an unstable nucleus, with atomic number Z and N, decays to a nucleus with $Z \pm 1$ and $N \mp 1$ and emits an electron (positron) and an anti-neutrino (neutrino). In β decay the atomic number $A = Z + N$ is unchanged. There are three types of beta decay:

1. β^- decay occurs when in a nucleus a neutron changes into a proton with the emission of an electron and an anti-neutrino;
   $n \rightarrow p + e^- + \bar{\nu_e}$,
   ${}^A_Z X \rightarrow {}^A_{Z+1} Y + e^- + \bar{\nu_e}$.

2. β^+ decay occurs when in a nucleus one proton changes into a neutron with the emission of a positron and a neutrino;
   $p \rightarrow n + e^+ + \nu_e$,
   ${}^A_Z X \rightarrow {}^A_{Z-1} Y + e^+ + \nu_e$.

3. Electron capture (EC) competes with β^+ decay and occurs when one of the atomic orbital electrons is captured by the nucleus and an electron neutrino is emitted;
   $p + e^- \rightarrow n + \nu_e$,
   ${}^A_Z X + e^+ \rightarrow {}^A_{Z-1} Y + \nu_e$.

For nuclear β or EC decay the Q value, or energy released in the decay process, can be expressed in terms of the atomic mass differences:

$$Q_{\beta^-} = [m({}^A_Z X) - m({}^A_{Z+1} Y)]c^2, \tag{1.1}$$

$$Q_{\beta^+} = [m({}^A_Z X) - m({}^A_{Z-1} Y)]c^2 - 2mc^2, \tag{1.2}$$

$$Q_{EC} = [m({}^A_Z X) - m({}^A_{Z-1} Y)]c^2. \tag{1.3}$$

Decay of an unstable parent via β^+ and EC decay yields the same daughter nucleus. Nuclei in which β^+ decay is energetically possible may also undergo EC decay, however the reverse situation is sometimes forbidden. The phenomenon of beta decay indicates the existence of specific interactions between nucleons and electrons. As mentioned before, Pauli was the first to suggest that beta decay with electron emission must be accompanied by emission of another particle. In support of this hypothesis we can cite the following arguments:

1. The beta particle can be emitted with an energy less than the energy difference between the initial and final nuclei. It is assumed that the neutrino carries the excess energy .

2. All the spins of nuclei found experimentally with an odd number of nucleons are half. From the fact that the beta decay does not change the mass number A, it appears that the change in angular momentum corresponds to an integer multiple of $\hbar$. In this case, emission of a single electron would be impossible, and the simultaneous emission of electrons and neutrinos is consistent with this condition.

1.2.1 Fermi's theory of beta decay

The theory of beta decay was formed in 1935 by Enrico Fermi. It was derived by analogy with the quantum mechanical treatment of electromagnetism, the formation of photons associated with the coupling of charged particles with the electromagnetic field [4]. He imagined a four point interaction that happens in a single point in space-time. The starting point is Fermi's golden rule, which describes the rate of quantum transition. The decay probability per unit time is given by perturbation theory:

$$P_{i\to f} = \frac{2\pi}{\hbar}|\langle i|H|f\rangle|^2\rho(E_f), \tag{1.4}$$

where i, f, $\rho(E_f)$ are the initial state, final state and density of final states, respectively. E_f is the available energy of the transition, which equals in beta decay $E_e + E_\nu$ with the condition that recoil energy is neglected. The matrix element $\langle i|H|f\rangle$ contains information about the structure of the nucleus and the wave functions of the hadrons and leptons. The neutrino final states can be rewritten as the product of two elementary volumes in phase space:

$$\rho(E_f) = V^2\frac{(4\pi p_e^2 dp_e)(4\pi p_\nu^2 dp_\nu)}{(2\pi\hbar)^6}\delta(E_f - E_e - E_\nu). \tag{1.5}$$

The weak interaction, in contrast with the to electromagnetic or gravitational interactions, can be considered local to a good approximation, it occurs in the place of the nucleon decay with no dependance on distance. Fermi proposed to couple two current vectors at the same point of space-time through a contact

interaction. The hadronic current vector was defined as:

$$J_h^\mu = (\overline{p}\gamma^\mu n).$$

The lepton current vector contains the lepton field leading to the lepton current density:

$$J_l^\mu = (\overline{\nu}\gamma^\mu e),$$

where γ^μ denotes the Dirac matrices. Then one can write the Hamiltonian for β^+ and β^- decay (summed over all protons and neutrons), respectively:

$$H_{\beta^+} = \frac{G_F}{\sqrt{2}}(\overline{p}\gamma^\mu n)(\overline{e}\gamma_\mu \nu_e), \tag{1.6}$$
$$H_{\beta^-} = \frac{G_F}{\sqrt{2}}(\overline{n}\gamma^\mu p)(\overline{\overline{\nu_e}}\gamma_\mu e),$$

where G_F denotes Fermi's coupling constant.

1.2.2 Parity violation

The parity transformation consists of reflecting all of the coordinates of a system $\overrightarrow{r} \rightarrow -\overrightarrow{r}$. If the parity transformation does not change some equations, it may be concluded that the equations are invariant with respect to parity transformation. The Hamiltonians given by Eq. 1.6 are invariant under parity transformation. There are only five independent bilinear covariant expressions for a relativistic spinor with spin 1/2:

Scalar $\bar{\psi}\psi$,

Vector $\bar{\psi}\gamma^\mu\psi$,

Tensor $\bar{\psi}\sigma^{\mu\nu}\psi$,

Axial Vector $\bar{\psi}\gamma^\mu\gamma^5\psi$,

Pseudo-Scalar $\bar{\psi}\gamma^5\psi$,

where $\bar{\psi} = \psi^{\dagger}\gamma^0$, $\sigma^{\mu\nu} = i/2(\gamma^{\mu}\gamma^{\nu} - \gamma^{\nu}\gamma^{\mu})$ and $\gamma^5 = i\gamma^0\gamma^1\gamma^2\gamma^3$. Establishing which of these bilinear forms are responsible for the weak interaction took for the experimentalists and theoreticians quite some time. The correct linear combination of bilinear forms replacing the vector in Eq. 1.6 turned out to be Vector - Axial Vector, combination $\bar{\psi}\gamma^{\mu}(1-\gamma^5)\psi$. Parity violation comes from the fact that the behavior of the vector and axial vector currents under a parity transformation are different. The vector current changes sign under parity transformation whereas the axial vector does not. Adjusting Eq. 1.6:

$$\begin{aligned} H_{\beta^+} &= G_F(\overline{p}\gamma^{\mu}(\mathbf{1} - \lambda\gamma_5)n)(\overline{e}\gamma_{\mu}(\mathbf{1} - \gamma^5)\nu_e), \\ H_{\beta^-} &= G_F(\overline{n}\gamma^{\mu}(\mathbf{1} - \lambda\gamma_5)p)(\overline{\overline{\nu_e}}\gamma_{\mu}(\mathbf{1} - \gamma^5)e), \end{aligned} \tag{1.7}$$

where $\lambda \approx 1.26$.

1.2.3 Selection rules

The electron and neutrino wave functions in beta decay contain the exponent functions:

$$\begin{aligned} \psi_e &\propto exp(\frac{i\vec{p_e}\vec{r}}{\hbar}), \\ \psi_{\nu} &\propto exp(\frac{i\vec{p_{\nu}}\vec{r}}{\hbar}). \end{aligned} \tag{1.8}$$

Since the exponent argument is very small (e.g. an electron with kinetic energy of $1MeV$ has momentum $p/\hbar = 0.004fm^{-1}$) the wave function can be developed into a series:

$$exp(\frac{i\vec{p}\vec{r}}{\hbar}) \approx 1 + \frac{i\vec{p}\vec{r}}{\hbar} + ...$$

If the matrix element does not vanish when substituted for the wave function is a 1, such a transition is called an allowed transition. When the next successive element should be considered in developing, so the matrix element does not vanish, those decays are called a "once forbidden". The hadronic part of the Hamiltonian has to contain a term accounting for the annihilation of the neutron (proton) and the creation of a proton (neutron). This is realized by introducing an isospin

operator τ_+ such that the nuclear matrix element

$$|M_F|^2 = |\langle f| \sum_j \tau_+^j |i\rangle|^2, \tag{1.9}$$

where j enumerates the nucleons in the nucleus. This type of transition is called a Fermi transition. The second type are Gamow-Teller transitions, with nuclear matrix elements given by:

$$|M_{GT}|^2 = |\langle f| \sum_j \vec{\sigma}^j \tau_+^j |i\rangle|^2. \tag{1.10}$$

Selection rules for allowed transitions are connected with the conservation of angular momentum, isospin and parity. The first rule is strict because it arises from the assumption of space isotropy. The second one is related to the load independency of forces, which is only approximate. All selection rules are the direct results of the matrix elements Eq. 1.9 and Eq. 1.10. In the Fermi transition there are no operators dependent on space or spin, consequently there is no change of total angular momentum and parity. These selection rules are known as Fermi's selection rules, who introduced the law of interaction corresponding to element Eq. 1.9. The selection rules in this case are:

$$\Delta J = 0, \Delta T = 0 \quad \text{and} \quad \pi_i \pi_f = +1. \tag{1.11}$$

The selection rules corresponding to matrix element Eq. 1.10 are slightly different, they have been called Gamow-Teller selection rules. In this case the matrix element can lead to a change in the total spin of 1 unit with conservation of orbital angular momentum and parity. Gamow-Teller transition rules have the form:

$$\Delta J = 0, \pm 1 \Delta T = 0, \pm 1 \quad \text{and} \quad \pi_i \pi_f = +1, \tag{1.12}$$

with an additional condition forbidding transitions with:

$$J = 0 \rightarrow J = 0. \tag{1.13}$$

Chapter 2

Electron capture in H-like, He-like and Li-like ions

In this chapter the electron capture process in lithium-, helium- and hydrogen-like ions is discussed. The wave functions of ions, with the proper orbital momentum are built from nuclear and electronic parts. The electronic part is approximated by Dirac hydrogen-like spinors with some effective charge. An explicit form of ion wave functions for allowed transitions in the electron capture process is presented below .

2.1 Wave functions for H-like ion

The wave function of the initial (final) state for a H-like ion is built from the part describing the mother (daughter) nucleus and the electron (neutrino) part denoted below by the index (l). In the initial (final) state the nucleus has spin I $(I, I \pm 1)$ and is coupled with the electron (neutrino) to spin I$\pm$1/2

$$\begin{aligned} |I \pm \frac{1}{2}\rangle_H &= \sum_{i=-1/2}^{1/2} (\frac{1}{2}, i, I', M-i|I \pm \frac{1}{2}, M) \\ &\quad \times |I', M-i\rangle_N |\frac{1}{2}, i\rangle_l, \end{aligned} \tag{2.1}$$

where the index N denotes the mother or daughter nucleus with spin I' (for daughter nucleus spin $I' = I$ or $I' = I \pm 1$). The expression $(\frac{1}{2}, i, I', M-i|I \pm \frac{1}{2}, M)$ denotes the Clebsh-Gordan coefficient.

2.2 Wave functions for He-like ion

Initial wave function

The wave function of a He-like ion is constructed as a product of the nuclear part having spin I (with its projection M) and the singlet wave function of two electrons (e_1 and e_2) coupled together to spin 0

$$|I, M\rangle_{He} = |I, M\rangle_N \frac{|+\rangle^{1s}_{e_1}|-\rangle^{1s}_{e_2} - |-\rangle^{1s}_{e_1}|+\rangle^{1s}_{e_2}}{\sqrt{2}}, \tag{2.2}$$

where $|i\rangle^{1s}_{e_k}$ denote Dirac relativistic spinors for the $1s$ state in H-like ions with spin 1/2 [14] (Appendix A, Eq. 6). Spinor indexes i and k denote the sign of the spin projection and the electron ordering number, respectively.

Final wave function

When allowed decays are considered, the nuclear spin changes by $\Delta I = 0, \pm 1$. The final state wave function is a product of the daughter nucleus (with spin I or $I \pm 1$), remaining electron and emitted neutrino. However, the remaining electron and emitted neutrino are coupled to spin 0 or 1. It is assumed that the emitted neutrino has spin 1/2 and carries no orbital momentum. The electron and neutrino are described by relativistic spinors with spin 1/2 (Appendix A, Eq. 6). If the captured electron and neutrino are coupled to spin 1 the leptonic part of the final state can be written as

$$\begin{aligned}
|1, 1\rangle_{\nu,1e} &= |+\rangle^{1s}_{\nu}|+\rangle^{1s}_{e_1}, \\
|1, 0\rangle_{\nu,1e} &= \frac{1}{\sqrt{2}}(|+\rangle^{1s}_{\nu}|-\rangle^{1s}_{e_1}) + |-\rangle^{1s}_{\nu}|+\rangle_{e_1}, \\
|1, -1\rangle_{\nu,1e} &= |-\rangle^{1s}_{\nu}|-\rangle^{1s}_{e_1}.
\end{aligned} \tag{2.3}$$

The weak interaction operator must conserve the total angular momentum and its projection. Therefore, the wave function for the final state needs to have total spin I with projection M:

$$\begin{aligned} |I,M\rangle_{He} &= \sum_{i=-1}^{1}(1,i,I',M-i|I,M) \\ &\times |1,i\rangle_{\nu,1e}|I',M-i\rangle_N, \end{aligned} \tag{2.4}$$

where $I' = I$ or $I' = I \pm 1$. In the case where remaining electron and neutrino are coupled to spin 0, the wave function has the form:

$$|I,M\rangle_{He} = |0,0\rangle_{\nu,1e}|I,M\rangle_N. \tag{2.5}$$

2.3 Functions for Li-like ions

Initial wave function

The electronic ground state wave function of a lithium-like ion with spin 1/2 again can be expressed as the anti-symmetrized product of 1s and 2s normalized relativistic Dirac spinors $|-\rangle^{ns}$ [6, 14, 53],

$$|1/2,1/2\rangle_{3e} = \frac{\mathcal{A}[|+\rangle|-\rangle|+\rangle]}{\sqrt{6}}. \tag{2.6}$$

The antisymmetrization operator is denoted by $\mathcal{A}$. However, equation 2.6 can be rewritten in the following form:

$$\begin{aligned} |1/2,1/2\rangle_{3e} &= \frac{1}{\sqrt{3}}|1^1S_0,0\rangle_{1,2}|+\rangle_{e3}^{2s} \\ &-\frac{1}{\sqrt{6}}|2^1S_0,0\rangle_{1,2}|+\rangle_{e3}^{1s} \\ &+\frac{1}{\sqrt{6}}|2^3S_1,0\rangle_{1,2}|+\rangle_{e3}^{1s} \\ &-\frac{1}{\sqrt{3}}|2^3S_1,1\rangle_{1,2}|-\rangle_{e3}^{1s}, \end{aligned} \tag{2.7}$$

where the wave functions of the helium-like ion and the electron labelled by the index 3 are separated. The helium-like wave functions are defined as following:

$$
\begin{aligned}
|1^1S_0,0\rangle_{1,2} &= \frac{\mathcal{A}[|+\rangle^{1s}_{e1}|-\rangle^{1s}_{e2}]}{\sqrt{2}},\\
|2^1S_0,0\rangle_{1,2} &= \frac{\mathcal{A}[|+\rangle^{1s}_{e1}|-\rangle^{2s}_{e2}-|-\rangle^{1s}_{e1}|+\rangle^{2s}_{e2}]}{2},\\
|2^3S_1,0\rangle_{1,2} &= \frac{\mathcal{A}[|+\rangle^{1s}_{e1}|-\rangle^{2s}_{e2}+|-\rangle^{1s}_{e1}|+\rangle^{2s}_{e2}]}{2},\\
|2^3S_1,\pm1\rangle_{1,2} &= \frac{\mathcal{A}[|\pm\rangle^{1s}_{e1}|\pm\rangle^{2s}_{e2}]}{\sqrt{2}}.
\end{aligned}
\tag{2.8}
$$

The total wave function of a lithium-like ion is constructed from the electronic part, given by Eq. 2.6, and the nuclear part with orbital momentum I. Both parts are coupled to the total orbital momentum $I \pm 1/2$

$$
\begin{aligned}
|I\pm1/2,M\rangle_{Li} &= \sum_{i=-1/2}^{1/2}(1/2,i,I,M-i|I\pm1/2,M)\\
&\times\ |1/2,i\rangle_{3e}|I,M-i\rangle_N.
\end{aligned}
\tag{2.9}
$$

Final wave function

The Li-like ion (with Z protons) decays by nuclear electron capture into a He-like ion (with Z-1 protons) emitting a neutrino with spin 1/2. However, the He-like ion could be created in three final states: the ground state- 1^1S_0 or two excited states- 2^1S_0 and 2^3S_1. For the ground state of the He-like ion the total wave function has a simple form:

$$
\begin{aligned}
|I\pm1/2,M,2^1S_0\rangle_{He} &= \sum_{i=-1/2}^{1/2}(1/2,i,I\pm1,M-i|I\pm1/2,M)\\
\times|1^1S_0,0\rangle_{1e,2e}&|1/2,i\rangle_\nu|I\pm1,M-i\rangle_N.
\end{aligned}
\tag{2.10}
$$

For an excited, spherically symmetric 2^1S_0 He-like ion the final wave function can be constructed in a similar way:

$$|I \pm 1/2, M, 2^1S_0\rangle_{He} = \sum_{i=-1/2}^{1/2} (1/2, i, I \pm 1, M - i|I \pm 1/2, M) \times |2^1S_0, 0\rangle_{1e,2e}|1/2, i\rangle_\nu |I \pm 1, M - i\rangle_N. \quad (2.11)$$

The expression describing the excited electronic wave function with spin 1 has the form:

$$|I \pm 1/2, M, 2^3S_1, S\rangle_{He} = \sum_{n=-1/2}^{1/2} \sum_{i=-S}^{S} (S, i, I \pm 1, M - i|I \pm 1/2, M)(1, i - n, 1/2, n|S, i) \times |2^3S_1, i - n\rangle_{1e,2e}|1/2, n\rangle_\nu |I \pm 1, M - i\rangle_N. \quad (2.12)$$

One can observe that in this case the electron wave function can be coupled together with the neutrino to spin 1/2 or 3/2 (denoted in Eq. 2.12 as S).

2.4 Electron capture probability in H-like ions

The weak interaction operator $\hat{O}$, responsible for electron capture [16], acts on nuclear and leptonic variables involved in the process and has non-zero matrix elements only between states with identical total orbital momentum and its projection. The probability (per unit time) of the process is given by the formula:

$$P = \frac{2\pi}{\hbar} |\langle f|\hat{O}|i\rangle|^2 \rho_f. \quad (2.13)$$

A H-like ion consists of an atomic nucleus with spin I and a single bound electron with spin 1/2. The total initial spin F_i of the ground state depends on the sign of the magnetic moment. If it is positive (negative) the ground state total spin equals $F_i = I - 1/2$ $(F_i = I + 1/2)$. In electron capture, the parent nucleus with spin I decays to the daughter nucleus with spin $I \pm \Delta I$. The most probable orbital angular momentum of the outgoing neutrino is $\Delta I - 1$, in that case together with the daughter nucleus they can be coupled to total spins ranging from $I \pm 1/2$ to

$|I \pm 2\Delta I \mp 1| \pm 1/2$. Only transitions $F_i = I \pm 1/2 \rightarrow F_f = I \pm 1/2$ conserve total angular momentum. Thus there exist $2(I \pm 1/2) + 1$ initial states with different angular momentum projections and equal occupation probabilities [39]. The probability of EC decay in a hydrogen-like ion equals:

$$\begin{aligned} P_H^{\pm} &= \frac{2\pi\rho_f}{\hbar[2(I \pm 1/2) + 1]} \\ &\times \sum_M |_{N,\nu}\langle I \pm 1/2, M|\hat{O}|I \pm 1/2, M\rangle_H|^2, \end{aligned} \tag{2.14}$$

where $P_H^{\pm}$ is the EC probability of a H-like ion with spin $I \pm 1/2$, ρ_f is the density of neutrino final states, $|I \pm 1/2, M\rangle_H$ and $|I \pm 1/2, M\rangle_{N,\nu}$ describe the initial and final states, respectively.

2.5 Electron capture probability in He-like ions

The initial state of a He-like ion is taken to have the form of Eq. 2.2, where instead of Z an effective (screened) charge $Z' = Z - q$ is used. In the final state (f), the nuclear spin changes by ΔI units, meaning $I_f = I \pm \Delta I$. The remaining electron is described by a relativistic spinor with spin 1/2. The most probable case is when the neutrino carries away orbital momentum $\Delta I - 1$ and the neutrino angular momentum equals $\Delta I - 1/2$ or $\Delta I - 3/2$. However, only a neutrino with total angular momentum $\Delta I - 1/2$, the remaining electron with spin 1/2 and the nucleus with spin $I \pm \Delta I$ can be coupled to angular momentum I, so the basis of final states has the form

$$|M', k, l\rangle^{ns}_{N,\nu,1e} = |I \pm \Delta I, M'\rangle_N \otimes |\Delta I - 1/2, k\rangle_\nu \otimes |1/2, l\rangle^{ns}_{1e},$$

where M', k, l denote the projection of the angular momentum for the daughter nucleus, neutrino and the remaining electron in the bound state ns respectively. The expression describing the EC decay probability in a helium-like ion is:

$$\begin{aligned} P_{He} &= 2\frac{2\pi\rho'_f}{\hbar(2I+1)} \\ &\times \sum_{M,M',k,l,n} |^{ns}_{N,\nu,1e}\langle M', k, l|\hat{O}|I, M\rangle_{He}|^2, \end{aligned} \tag{2.15}$$

where ρ'_f denotes the density of neutrino final states in He-like ions and the factor 2 in front of the equation accounts for the two possibilities that the electron labelled as e_1 or e_2 can be captured by the nucleus. In the next step corrections for different neutrino densities (in final states) in He- and H-like ions are introduced (Eq. 2.24 in subsection 2.5.2 and Eq. 2.26 in subsection 2.5.3) into Eq. 2.15:

$$\begin{aligned} P_{He} &= 2\frac{2\pi\rho_f}{\hbar(2I+1)}(1-\delta_1+\frac{\delta_2}{Q_{EC}}) \\ &\times \sum_{M,M',k,l,} |_\nu\langle \Delta I-1/2,k|_N\langle I\pm\Delta I,M'|\hat{O}|I,M\rangle_N|1/2,l\rangle_{2e}|^2. \end{aligned} \tag{2.16}$$

Nuclear states and captured electron states (denoted as 2e) from Eq. 2.16 form the basis $|I,M\rangle_N|1/2,l\rangle_{2e}$ with $2(2I+1)$ independent vectors which can be expanded in the basis of H-like ion states with fixed angular momenta: $|I+1/2,m\rangle_H$ and $|I-1/2,m\rangle_H$. Both of these two bases have an identical number of $2(2I+1)$ vectors. Similarly in the case of final states, $|I\pm\Delta I,M'\rangle_N|\Delta I-1/2,k\rangle_\nu$ can be expanded into $2\Delta I-1$ separate bases with fixed angular momenta: $|I\pm1/2,m\rangle_{N\nu}$, $|I\pm3/2,m\rangle_{N\nu}$, ... However, the weak interaction operator $\hat{O}$ has nonzero matrix elements only between states with identical total angular momentum and its projection, therefore in this case an equality can be written as:

$$\begin{aligned} &\sum_{M,M',k,l,} |_\nu\langle \Delta I-1/2,k|_N\langle I\pm\Delta I,M'|\hat{O}|I,M\rangle_N|1/2,l\rangle_{2e}|^2 \\ &= \sum_m |_{N,\nu}\langle I\pm1/2,m|\hat{O}|I\pm1/2,m\rangle_H|^2. \end{aligned} \tag{2.17}$$

The electron spinors in Eq. 2.17 employ an effective charge Z'. Taking Eqs. 2.14, 2.16, 2.17 and expressing the electron density at the nucleus in terms of relativistic spinors with charge Z', the final relation takes the form:

$$\begin{aligned} P_{He} = \quad & \frac{[2(I\pm1/2)+1]}{2I+1}P_H \\ & \times(1-\delta_1+\frac{\delta_2}{Q_{EC}})(1-\frac{5}{16Z})^3(1+\delta_3), \end{aligned} \tag{2.18}$$

where the corrections δ_1, δ_2, δ_3 denote the probability that the remaining electron is unbound, decay energy correction and relativistic screening correction respec-

tively. In Table 2.1 the corrections are listed. The screening correction has the biggest influence on the value of the probability ratio. It can reach for He atoms approximately 60%.

Z	q	$(1-\frac{5}{16Z})^3$	$log_{10}(\delta_1)$	$\delta_2(keV)$	$\delta_3 \cdot 10^{-2}$
2	0.312	0.601	-0.87	0.0	-0.06
12	0.312	0.924	-2.86	-0.2	-0.25
22	0.309	0.958	-3.41	-0.4	-0.41
32	0.306	0.971	-3.73	-0.6	-0.54
42	0.301	0.978	-3.94	-0.8	-0.66
52	0.294	0.982	-4.09	-1.1	-0.78
62	0.286	0.985	-4.19	-1.3	-0.88
72	0.275	0.987	-4.26	-1.5	-0.98
82	0.263	0.989	-4.29	-1.8	-1.07
92	0.247	0.990	-4.29	-2.1	-1.15

Table 2.1: The screening factor $q = Z' - Z$ and the corrections δ_1, δ_2 and δ_3 listed for selected nuclei. Z denotes an atomic number.

2.5.1 Screening correction

In the present subsection the influence of the Coulomb interaction between two electrons or the so-called screening correction on the probability ratio is calculated. The wave function of two electrons is approximated by two Dirac spinors 1s coupled to spin 0 with an effective charge $Z' = Z - q$, where q is a free parameter. The value of the effective charge is derived from the minimized expectation value of $E(Z, Z') = \langle 0|H|0\rangle$, where H is the Hamiltonian taken for two interacting electrons in the potential of a point-like nucleus with charge Z. An analytical expression for $E(Z, Z')$ has been obtained in the form (derivation given in Appendix

B):

$$E(Z,Z') = 2\sqrt{1-\alpha^2 Z'^2} + \frac{2\alpha^2 Z'(Z'-Z)}{\sqrt{1-\alpha^2 Z'^2}} + \frac{\alpha^2 Z' \left(\sqrt{1-\alpha^2 Z'^2} - \frac{4^{-2\sqrt{1-\alpha^2 Z'^2}} \Gamma\left(4\sqrt{1-\alpha^2 Z'^2}\right)}{\Gamma\left(2\sqrt{1-\alpha^2 Z'^2}\right)^2} \right)}{1-\alpha^2 Z'^2}, \tag{2.19}$$

where α is the fine-structure constant. The screening parameter q is plotted in Fig. 2.1. The parameter q in the non-relativistic limit is independent of Z and equals 5/16 [39].

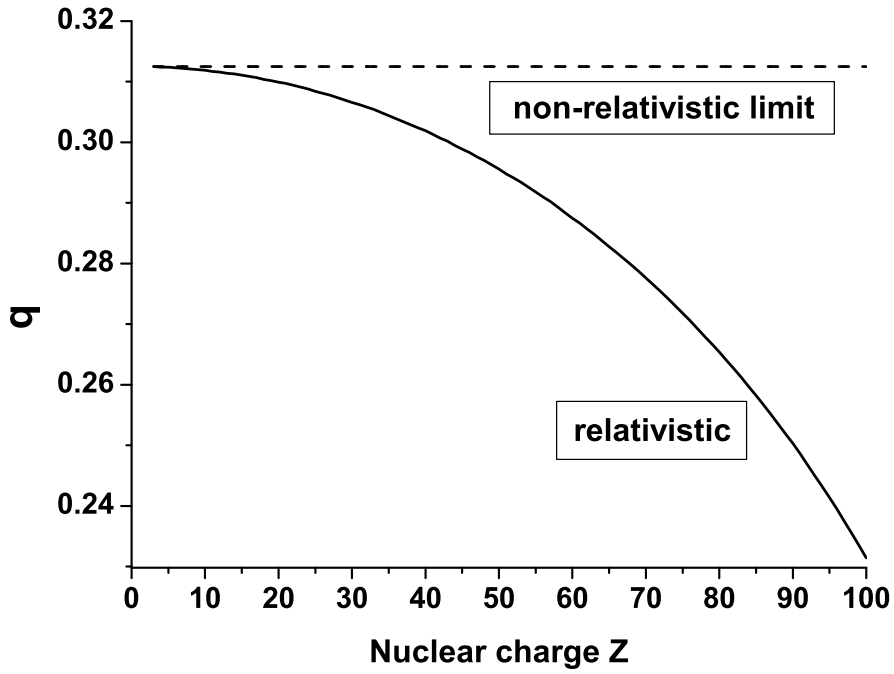

Figure 2.1: The relativistic screening parameter q plotted as a function of the nuclear charge Z. The non-relativistic limit, independent of Z, is $q = 5/16$ [39].

The ratio of non-relativistic electron densities at r=0 (in the nucleus) between He- and H-like ions is given by the simple equation [39]:

$$\frac{\rho_{He}}{\rho_H} = 2(1 - \frac{5}{16Z})^3. \tag{2.20}$$

In Figure 2.2 the evaluation of the electron densities ratio is shown. However, for

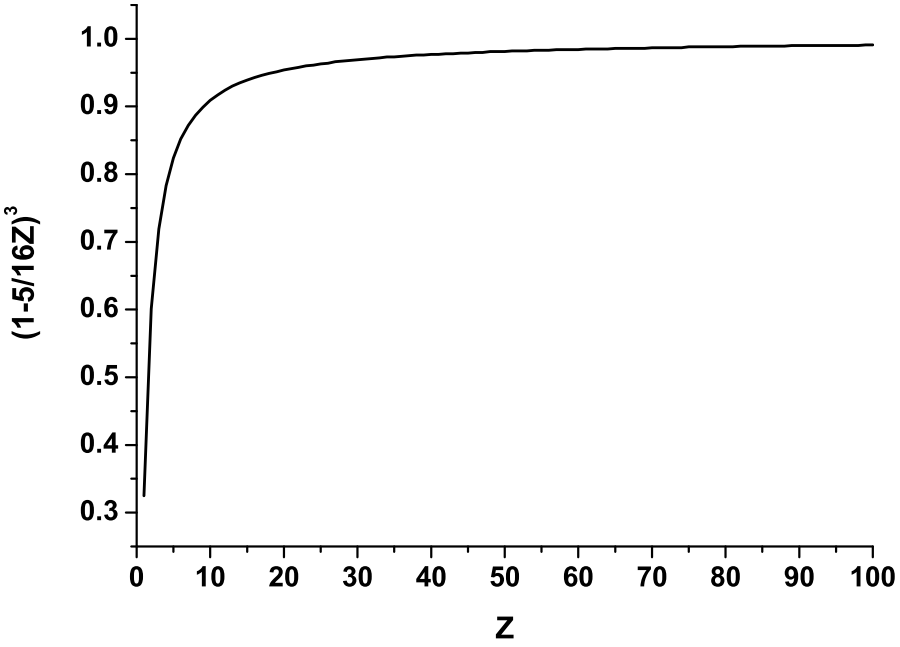

Figure 2.2: The screening correction $(1-\frac{5}{16Z})^3$ plotted as a function of the nuclear charge Z. [39].

a relativistic density the relation can not be applied because the Dirac spinor 1s is divergent for r=0 and the ratio does not exist. Therefore, the electron density has been averaged over the nuclear volume with radius $R_a = 1.24A^{1/3}$ fm,

$$\tilde{\rho_e}(Z) \equiv \frac{3}{R_a^3}\int_0^{R_a}[f_{1s}(r,Z)^2 + g_{1s}(r,Z)^2]r^2dr. \tag{2.21}$$

Note, that the relativistic density multiplied by r^2 is not divergent at $r = 0$. Takin Eq. 2.21 in advantage the relativistic density ratio can be written as:

$$\frac{\rho_{He}}{\rho_H} = 2(1-\frac{5}{16Z})^3(1+\delta_3), \tag{2.22}$$

where the correction δ_3 is given by the expression:

$$\delta_3 = \frac{\tilde{\rho_e}(Z-q)}{(1-\frac{5}{16Z})^3\tilde{\rho_e}(Z)} - 1. \tag{2.23}$$

The correction δ_3 shows how big an influence relativistic effects can have on the electron density in the nucleus. One can observe that the calculated absolute value of δ_3 is smaller than 0.012 (see Fig. 2.3).

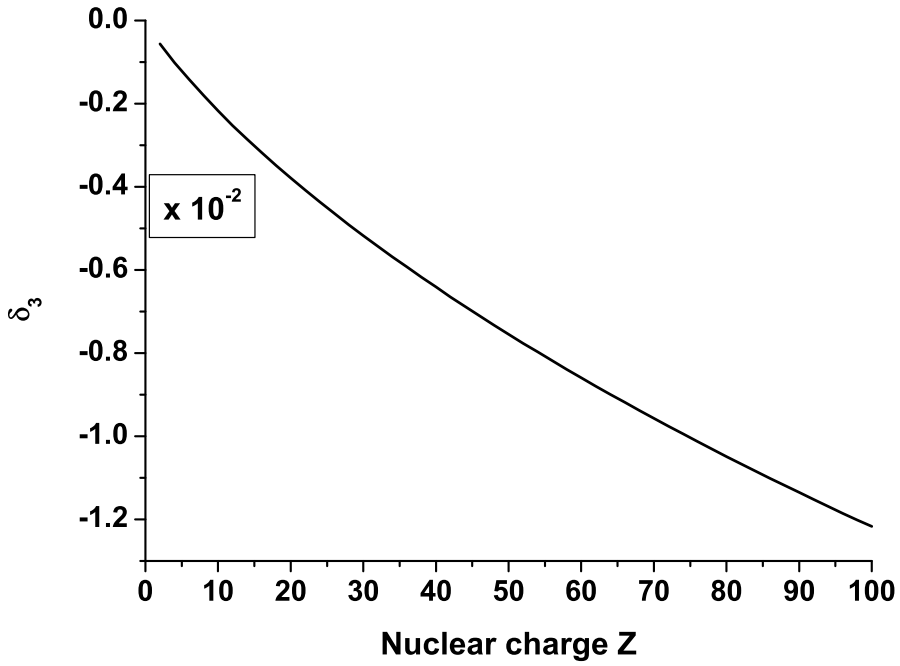

Figure 2.3: The relativistic correction δ_3 as a function of the nuclear charge Z.

2.5.2 Probability that the remaining electron is unbound

We discuss a new electron capture decay channel in a helium-like ion accompanied by the emission of the remaining electron into the continuum. This is a very exotic type of Auger electron emission. The ionization probability for the new decay channel is calculated. The sum of the ionization probability and the probability that the remaining electron is bound in a H-like ion equals unity. Therefore, the ionization probability can be estimated from the expression:

$$\delta_1 = 1 - \sum_n |\langle ns, Z-1 | 1s, Z-q \rangle|^2, \tag{2.24}$$

where the summation is over all ns bound states in the H-like ion. The ioniza-

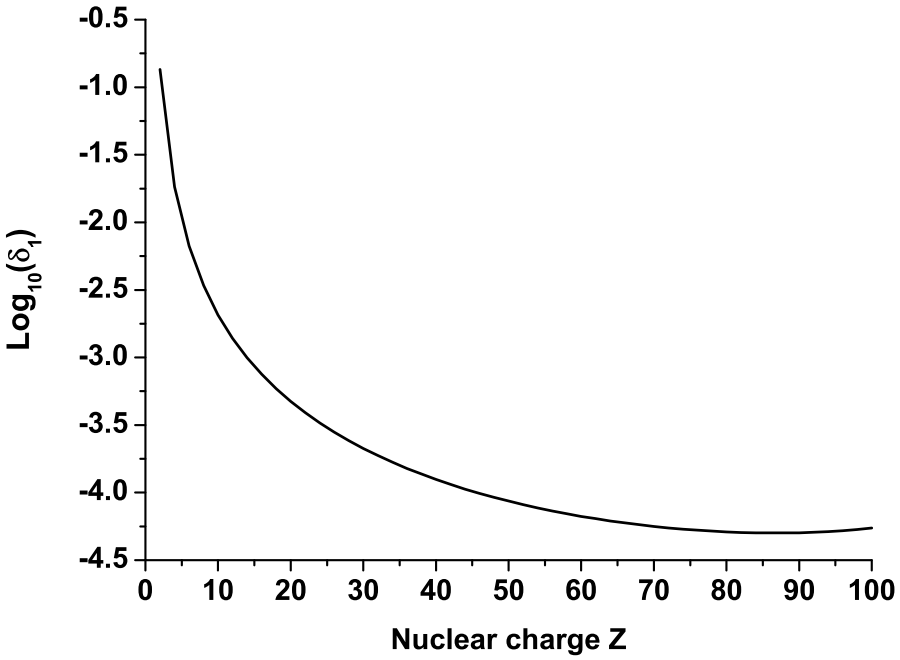

Figure 2.4: The ionization probability δ_1 (an a logarithmic scale) in the electron capture process of a He-like ion plotted as a function of atomic number Z.

tion probability reaches a value of about 0.1 for light nuclei and monotonically decreases down to 5.6×10^{-5} for Pb isotopes, see Fig. 2.4.
The ionization probability in electron capture of helium-like ions has not been tested experimentally. However, a similar process in the beta decay of He ions is discussed in the next chapter.

2.5.3 Different densities of final states

The densities of the neutrino final states in electron capture of He-like and H-like ions differ due to the different decay energies for both types of ions. The ratio of the two neutrino densities takes the form:

$$\frac{\varrho_f^{He^2}}{\varrho_f^{H^2}} = \frac{(Q_{EC} + \delta Q_n)^2}{Q_{EC}^2},$$

$$\frac{\varrho_f^{He}}{\varrho_f^{H}} \approx 1 + 2\frac{\delta Q_n}{Q_{EC}},$$

where the quantity Q_{EC} denotes the mass difference between mother H-like ion and the daughter bare nucleus. The quantity δQ_n is the difference in electron capture energy between the He-like ion and an excited ns state of the H-like ion [12, 35]

$$\delta Q_n = Q_{EC}^{He} - Q_{EC}^{H} = B_1^{1s}(Z) + B_1^{ns}(Z-1) - B_2(Z), \tag{2.25}$$

where $B_1^{ns}(Z)$ denotes the binding energy of an electron in the bound state ns of the H-like ion with the nuclear charge Z. The total ionization energy $B_2(Z)$ of the He-like ion was taken from the paper [12]. The quantity δQ_n is a decreasing function of atomic number Z and is equal to -0.1 keV for Z=10 and reaches -0.8 keV for Z=73. The value of δQ_n is typically smaller than the experimental uncertainties of Q_{EC}. The correction δ_2 equals the quantities $2\delta Q_n$ averaged over the probabilities $|\langle ns, Z-1|1s, Z-q\rangle|^2$ to reach the ns bound state in the H-like ion

$$\delta_2 = 2\sum_n |\langle ns, Z-1|1s, Z-q\rangle|^2 \delta Q_n. \tag{2.26}$$

The correction δ_2 varies from $-0.2\ keV$ for $Z = 12$ up to $-2.1\ keV$ for $Z = 92$ and is listed in Table 2.1.

2.5.4 Arbitrary neutrino orbital momentum

In the preceding subsections we have discussed electron capture assuming that the neutrino is emitted without orbital angular momentum. In the present section the discussion is extended to the case when the neutrino takes an orbital momentum less then or equal to ΔI. Thus, both hyperfine states $I \pm 1/2$ of the H-like ion can decay with the probabilities denoted by $P_H^{\pm}$, respectively. In a similar way as in the previous section it can be demonstrated that the following relation holds combining the electron capture probabilities for He-like and H-like ions and there

exists a relationship:

$$P_{He} = [\frac{2(I+\frac{1}{2})+1}{2I+1}P_{H^+} + \frac{2(I-\frac{1}{2})+1}{2I+1}P_{H^-}] \times(1-\delta_1+\frac{\delta_2}{Q_{EC}})(1-\frac{5}{16Z})^3(1+\delta_3) \tag{2.27}$$

For the transition $I \rightarrow I-1$ the probabilities $P_H^{\pm}$ satisfy the relation

$$\frac{P_H^+}{P_H^-} \approx (kR)^2, \tag{2.28}$$

where k denotes the neutrino momentum (divided by $\hbar$) and R is the average nuclear radius. For the transition $I \rightarrow I+1$ the latter equation should be inverted. Assuming $Q_{EC} = 5$ MeV and R = 5 fm, we get $(kR)^2$ =0.016.

2.5.5 Astrophysical applications

The creation of the light elements D, ^{3}He and Li was the major event in the Universe after the Big Bang and the inflation stage. It has an influence on our everyday life on earth. Creation of deuterium from a neutron and a proton is the first step in the nuclear reaction chain. When the temperature of the Universe was about 0.1 MeV Big Bang nucleosynthesis (BBN) started.
We give a short discussion of ^{7}Be and its decay to ^{7}Li in BBN. A bare nucleus of beryllium recombined with an electron decays by electron capture through the following reactions:

$$^7Be + e^- \rightarrow ^7 Li + \nu_e \tag{2.29}$$

or

$$^7Be + e^- \rightarrow ^7 Li^* + \nu_e \qquad ^7Li^* \rightarrow ^7 Li + \gamma \tag{2.30}$$

where $^7Li^*$ is the excited state of the lithium nucleus with an energy of 477.6 keV. The Q-value of the reaction is 861.8 keV [67]. The half life value for a neutral atom of ^{7}Be equals 53.2 days and the second reaction occurs with a probability of

10.44 %. The experimental spin values for ^{7}Be, ^{7}Li, ^{7}Li* are assigned to be 3/2, 3/2 and 1/2, respectively (see Fig. 2.5).

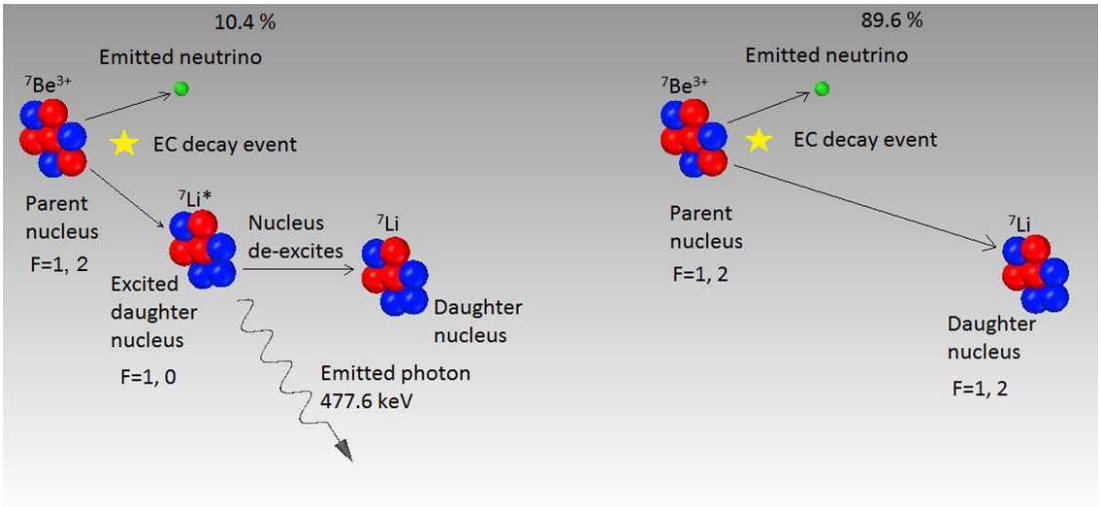

Figure 2.5: Effect of hyperfine splitting of $^7Be^{3+}$ on nuclear reactions.

In the first reaction 2.29 the initial and final spins are equal to 3/2 and we have the relation between decay probabilities for $P_{Be^{2+}}$ and $P_{Be^{3+}}$

$$P_{Be^{2+}} = [\frac{2(I-\frac{1}{2})+1}{2I+1}P^-_{Be^{3+}} + \frac{2(I+\frac{1}{2})+1}{2I+1}P^+_{Be^{3+}}] \times(1-\delta_1+\frac{\delta_2}{Q_{EC}})(1-\frac{5}{16Z})^3(1+\delta_3) \tag{2.31}$$

However, at high temperatures the hyperfine states with spins I$\pm$1/2 are populated with statistical weights $\frac{2(I\pm\frac{1}{2})+1}{2(2I+1)}$ and the total probability of electron capture for Be^{3+} equals

$$P_{Be^{3+}} = [\frac{2(I-\frac{1}{2})+1}{2I+1}P^-_{Be^{3+}} + \frac{2(I+\frac{1}{2})+1}{2I+1}P^+_{Be^{3+}}]. \tag{2.32}$$

Combining the two equations 2.31 and 2.32:

$$P_{Be^{2+}} = P_{Be^{3+}}(1-\delta_1+\frac{\delta_2}{Q_{EC}})(1-\frac{5}{16Z})^3(1+\delta_3). \tag{2.33}$$

It can be demonstrated that a similar relation holds for the second reaction with spin transition $3/2 \rightarrow 1/2$ between ^{7}Be and ^{7}Li*. In the paper by Khatri and Sunyaev [37] it is estimated that in the hot environment of the early Universe the ratio $P_{Be^{+2}}/P_{Be^{+3}} = 2$. However, the corrections, especially important for light nuclei, worked out in this thesis improve the Khatri and Sunyaev finding. Finally, the ratio is smaller than 2 and equal $P_{Be^{+2}}/P_{Be^{+3}} = 1.57$.

2.6 Electron capture in Li-like ions

In the present section we study electron capture in Li-like ions transiting to He-like ions in the ground state or one of two excited states. The formation of excited states in He-like ions is the subject of many experimental and theoretical studies [38, 58, 68]. He-like ions are the simplest multi-electron systems in nature. Investigation of these species has attracted the attention of theoreticians and experimentalists for some time.

2.6.1 Population of excited states in He-like ions

The probability that a Li-like ion with spin I in the allowed electron capture transition $I \rightarrow I \pm 1$ populates the 2^1S_0 excited state in a He-like ion is denoted by P_0:

$$\begin{aligned} P_0 &\propto {}_{3He}\langle I \pm 1/2, M, 2^1S_0|\hat{O}|I \pm 1/2, M\rangle^2_{Li} \\ &= \frac{1}{2}(1-\frac{q}{Z})^3{}_B\langle I \pm \frac{1}{2}, M|\hat{O}|I \pm \frac{1}{2}, M\rangle^2_H, \end{aligned} \tag{2.34}$$

where the initial and final wave functions are defined by Eq. 2.9 and 2.11. However, due the electron-electron interaction in a Li-like ion the effective charge in the 1s and 2s wave functions equals $Z - q$, with $q = 0.464$.
In a similar way the probability P_1 to reach the 2^3S_1 state in a He-like ion can

be estimated:

$$\begin{aligned} P_1 &\propto {}_{3He}\langle I \pm 1/2, M, 2^3S_1, 1/2|\hat{O}|I \pm 1/2, M\rangle^2_{Li} \\ &+ {}_{3He}\langle I \pm 1/2, M, 2^3S_1, 3/2|\hat{O}|I \pm 1/2, M\rangle^2_{Li} \\ &= \frac{2(I \pm 1)+1}{2(2I+1)}(1-\frac{q}{Z})^3{}_B\langle I \pm \frac{1}{2}, M|\hat{O}|I \pm \frac{1}{2}, M\rangle^2_H, \end{aligned} \tag{2.35}$$

where the expression has been summed over two possible couplings 1/2 and 3/2 of the 2^3S_1 excited state with the neutrino having spin 1/2.
The factor 3 in the front of Eqs. 2.34 and 2.35 reflects the 3 possibilities of electron capture in a Li-like ion. Finally, the ratio of probabilities P_0 and P_1 is given by the simple expression:

$$\frac{P_0}{P_1} = \frac{2I+1}{2(I \pm 1)+1}. \tag{2.36}$$

A few examples of the $\frac{P_0}{P_1}$ ratio are calculated in Table 2.2. As can be seen, the most effective way to reach the 2^1S_0 state in a helium-like ion is electron capture with the nuclear transition $1 \rightarrow 0$. The probability to reach the ground

I	$\frac{P_0}{P_1}$ $I \rightarrow I-1$	$\frac{P_0}{P_1}$ $I \rightarrow I+1$
0		$\frac{1}{3}$
$\frac{1}{2}$		$\frac{1}{2}$
1	3	$\frac{3}{5}$
$\frac{3}{2}$	2	$\frac{2}{3}$
...	...	...
∞	1	1

Table 2.2: The ratio of probabilities P_0/P_1 that a Li-like ion decays into the 2^1S_0 and 2^3S_1 excited states of a He-like ion. The ratio is calculated for two types of EC decays $I \rightarrow I \pm 1$.

state can be calculated just like the probability P_0. However, in this case the

electron is captured from the 2s orbital instead of the 1s. Therefore, the ratio of probabilities to reach the 1^1S_0 and 2^1S_0 states equals the ratio of the electron densities $\rho_e^{2s}(Z)/\rho_e^{1s}(Z)$ at the nucleus. The electron density averaged over the nuclear volume was calculated from formula 2.21 taken for 1s and 2s states.
The calculated ratio $\rho_e^{2s}(Z)/\rho_e^{1s}(Z)$ is plotted in Fig. 2.6. The 1^1S_0 ground state

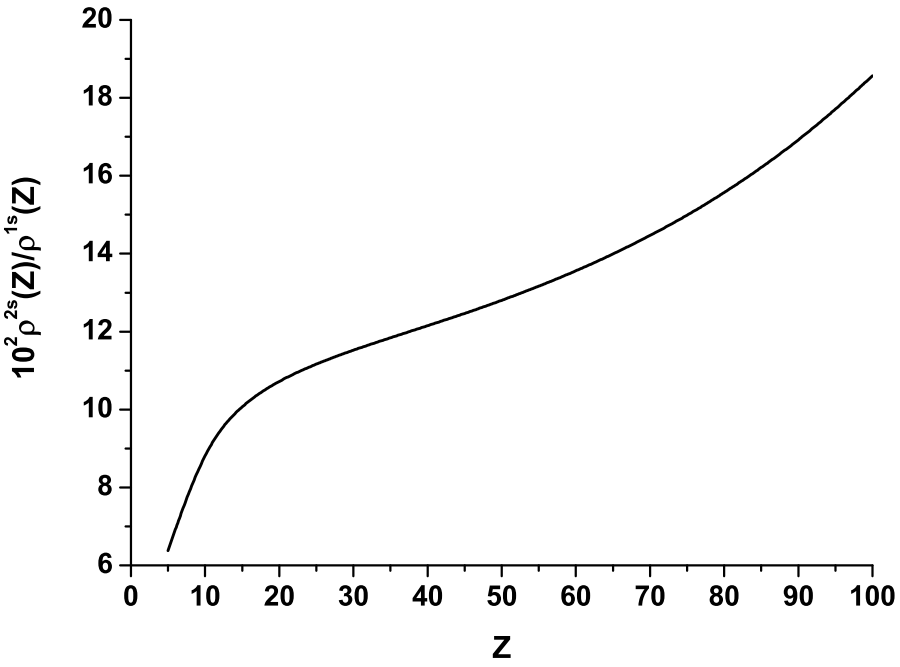

Figure 2.6: The ratio of the two densities $\rho^{2s}(Z)$ and $\rho^{1s}(Z)$ for 2s and 1s hydrogen-like relativistic states in the Coulomb field with charge Z is plotted. The average electron density at the nucleus is calculated according Eq. 2.21. In the non-relativistic limit, the ratio has the constant value 0.125. The plotted ratio is multiplied by a factor of 100.

population probability for light elements is almost 16 times smaller than the corresponding probability for the 2^1S_0 excited state. For the heaviest elements, the ratio approaches value of 0.18. In the non-relativistic limit the ratio is constant and equals 0.125.
The electron initial wave function in a Li-like ion can be expanded in the basis of the ground state and two excited states in a He-like ion. However, the He-like wave functions are constructed from H-like 1s and 2s states. It is assumed that

two states 1s and 2s in the Coulomb fields of Z and Z-1 protons are orthogonal. This assumption has been tested calculating numerically the matrix elements:

$$
\begin{aligned}
&{}_{Z-1} < 2s|1s >_Z \equiv \\
&\int_0^\infty (f_{2s,Z-1}(r) f_{1s,Z}(r) + g_{2s,Z-1}(r) g_{1s,Z}(r)) r^2 dr,
\end{aligned}
\tag{2.37}
$$

and the obtained values of the matrix elements for Z equal to: 5, 60 and 90 are 0.105, 0.011 and 0.009, respectively.

The matrix elements ${}_{Z-1}\langle 2s|1s\rangle_Z$ are plotted in Figure 2.7 as a function of Z.

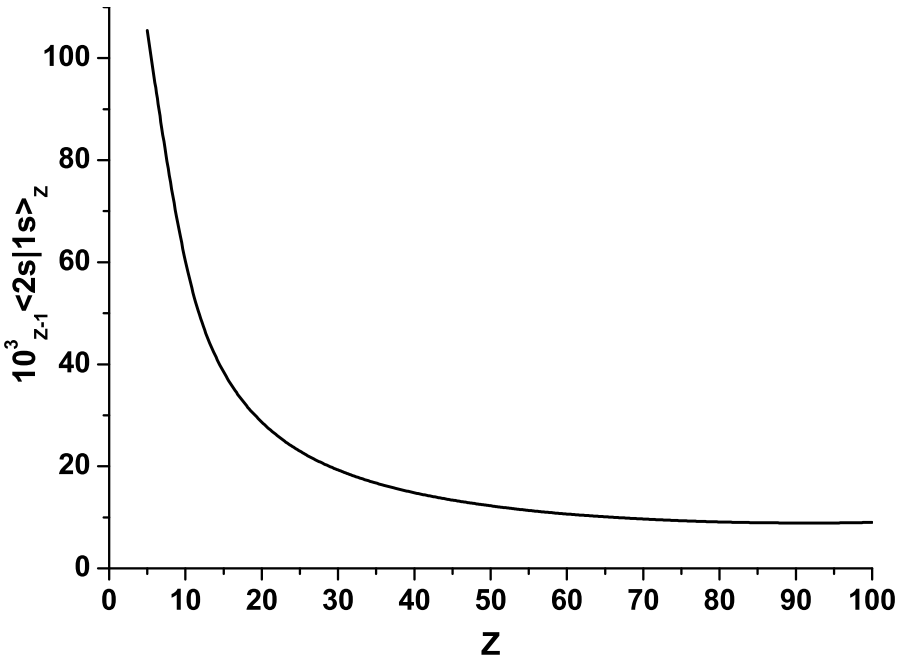

Figure 2.7: The matrix elements ${}_{Z-1}\langle 2s|1s\rangle_Z$ calculated for two relativistic spinors 1s and 2s as a function of atomic number Z (multiplied by 1000).

The matrix elements decrease with increasing atomic number Z and reach nearly 0.009 for nuclei close to Uranium.

2.6.2 Ratio of electron capture probabilities for Li- and H-like ions

By P_{Li} is denoted the electron capture probability in Li-like ions. For allowed transitions $I \rightarrow I+1$ $(I \rightarrow I-1)$ in a Li-like ion, it is assumed that Li-like ions are initially in states with spin $I \rightarrow I+1/2$ $(I \rightarrow I-1/2)$, respectively. Then the probability P_{Li} equals the sum of probabilities that the lithium-like ion decays into the 1^1S_0 ground state and 2^1S_0, 2^3S_1 excited states. The probability of EC decay into the ground state is proportional to $P_0 \frac{\rho^{2s}(Z)}{\rho^{1s}(Z)}$. Summing up the three probabilities P_0, P_1, given by equations 2.34 and 2.35, and the probability to reach the ground state simple the following relation is obtained:

$$P_{Li} = (\frac{2(I \pm 1/2)+1}{(2I+1)} + \frac{\rho^{2s}(Z)}{2\rho^{1s}(Z)})(1-\frac{q}{Z})^3 P_H, \tag{2.38}$$

where $P_H \propto {}_B\langle I \pm \frac{1}{2}, M|\hat{O}|I \pm \frac{1}{2}, M\rangle_H^2$. The ratio of densities $\rho^{2s}(Z)/\rho^{1s}(Z)$ is plotted in Fig. 2.6 and varies from 0.06 for the light nuclei up to 0.20 for the heaviest ones.

In the allowed EC transition $I \rightarrow I+1$ $(I \rightarrow I-1)$, due to the conservation of the total orbital momentum a hydrogen-like ion decays only from a state with spin equal to $I+1/2$ $(I-1/2)$, respectively. However, a lithium-like ion, contrary to the case of a hydrogen-like ion, can also decay from the state $I-1/2$ $(I+1/2)$. This is allowed, because the 2^3S_1 helium excited state couples with a neutrino to spin 3/2. Both states can then be coupled with the spin of the daughter nucleus $I+1$ $(I-1)$ to total spin $I-1/2$ $(I+1/2)$, respectively. The probability that in the allowed EC transition $I \rightarrow I+1$ $(I \rightarrow I-1)$, a lithium-like ion decays from the state $I-1/2$ $(I+1/2)$ is denoted as P'_{Li}. It can be expressed by the decay probability of a hydrogen-like ion P_H:

$$P'_{Li} = \frac{2(I \pm 1/2)+1}{(2I+1)}(1-\frac{q}{Z})^3 P_H. \tag{2.39}$$

The relation obtained is similar to Eq. 2.38. However, it does not depend on the ratio of electron densities.

2.6.3 Experimental applications

The results obtained in the current chapter can be widely applied in designing experiments for determining the relative probability of electron capture for H-like, He-like and Li-like ions.

As an interesting possibility is a measurement of the spin of the mother nucleus of a decaying Li-like ion. Spin measurement is especially important for short-lived, neutron-deficient nuclei, which mostly have unmeasured ground state spin values. Assuming an electron capture transition of the $I \rightarrow I \pm 1$ type and measuring in the experiment the ratio P_0/P_1, the spin of the mother nucleus can be experimentally determined using Eq. 2.36.

Another interesting possibility is a measurement of the ratio of 1s and 2s densities at the nucleus. As an example using Eq. 2.38 one can assume the electron capture transition $1 \rightarrow 0$ occurring for some nuclei in the vicinity of Z=60. For a specified transition the ratio equals $P_{Li}/P_H = 0.98(2/3 + \delta)$, where $\delta = \rho^{2s}(Z)/\rho^{2s}(Z) \approx 0.075$ for Z=60.

Chapter 3

Electron capture in H-like and He-like ions- experiment

The formulas obtained in the previous chapter can be successfully used in various experiments related to electron capture. Modern electron capture probabilities are measured with uncertainties near 1%. The transition probabilities for hydrogen- and helium-like ions for ^{142}Pm, ^{140}Pr and hydrogen-like only for ^{122}I were measured at the GSI Darmstadt facility. In this chapter the experimental status will be outlined and a short comparison made with the theoretical results.

3.1 Experimental setup

Progress in experimental techniques in recent years, based on projectile fragmentation, in-flight separation and heavy-ion storage rings has enabled investigations of beta-decay of highly-charged ions [7, 26, 33, 36, 41, 51]. Currently only two facilities in the world are capable of producing beams of radioactive nuclei in high atomic charge states and to store them for extended periods of time [46]. One of them is FRS-ESR at GSI-Darmstadt and the second is HIRFL-CSR at IMP in Lanzhou, China. However, the experiments at IMP are still in the planning phase while the experimental program at GSI has been running for about two decades. Recently, using the so-called time-resolved Schottky Mass Spectrometry (SMS) [42, 43, 54, 55] at GSI Darmstadt the first experiments on orbital electron capture

decay of few-electron ions have been performed. Here the corresponding in-flight fragment separators FRS [27] and RIBLL2 [73] are coupled to the cooler-storage rings ESR [20] and CSRe [74], respectively (see Fig. 3.1).

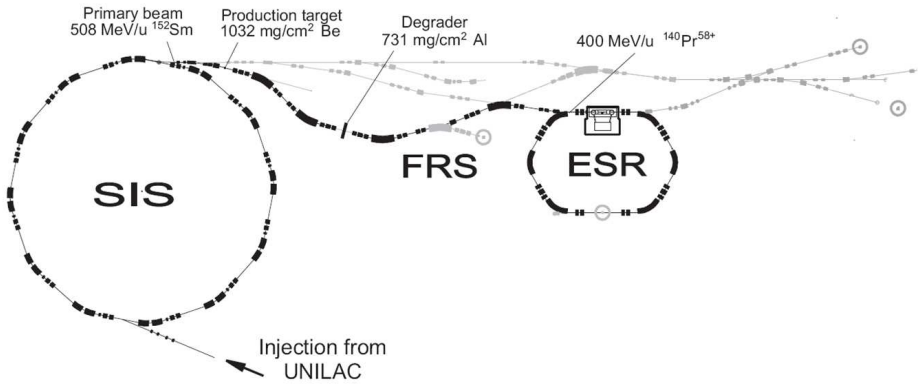

Figure 3.1: Schematic diagram showing a part of the high energy setup at the GSI Darmstadt facility, where SIS- denotes the heavy ion synchrotron, FRS- the fragment separator, ERS- the experimental storage ring.

ESR

The experimental storage ring ESR [21] presented in Fig. 3.1 has a circumference of about 108.36 m. It is equipped with an electron and stochastic cooling system, a gas jet target, various detectors and mechanical slits. The average ultra-high vacuum pressure is typically about 10-11 mbar. Beam lifetimes of up to several hours are attained, depending on the charge state of the stored ions and the electron cooler beam current.

SMS-Schottky Mass Spectrometry

Two techniques have been developed at the ESR for mass measurement of exotic nuclei: Schottky Mass Spectrometry (SMS) [22] and Isochronous Mass Spectrometry (IMS) [31]. Both are used as a highly sensitive and non-destructive beam diagnosis. The revolution frequency difference between two different ion species $\Delta f/f$ having a mass-to-charge ratio difference $\Delta(m/q)/(m/q)$ and a velocity

spread difference $\Delta v/v$ is given by equation [63]:

$$\frac{\Delta f}{f} = \frac{1}{\gamma_t^2}\frac{\Delta(m/q)}{m/q} + \frac{\Delta v}{v}(1 - \frac{\gamma^2}{\gamma_t^2}), \tag{3.1}$$

where γ is the Lorentz factor and γ_t^2 express the optical parameter of the ring. In order to have a direct relation between revolution frequency and mass-to-charge ratio the SMS and IMS exploit relation 3.1, by elimination of the second term. In the first case by reduction of the velocity spread and in the second case setting the Lorentz factor to $\gamma^2/\gamma_t^2 \rightarrow 1$.

A property of the time-resolved SMS is sensitivity to single-stored ions [43], which formed the basis for measuring individual electron capture decays of single H-like ions stored into the ESR. After injection in the ESR, the hot fragments

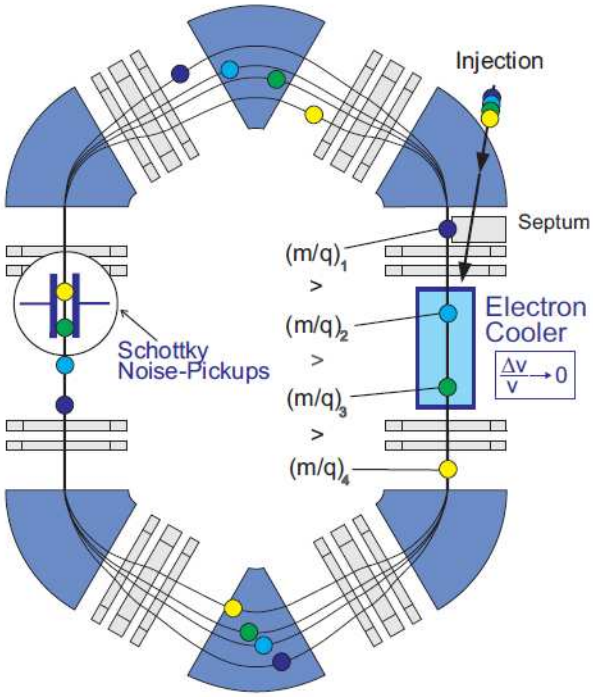

Figure 3.2: Schematic diagram showing a part of the ERS and SMS principle. The orbits of four differents ion species using four different colors are sketched. If all stored ions have the same velocity, then a specific revolution frequency is the signature of a specific mass-to-charge ratio.

coming from the FRS are first compressed in momentum by a stochastic pre-cooling system during the first seconds after injection [50]. Furthermore ions are cooled continuously by an electron cooler system [64] placed in one of the straight sections of the ESR lattice. The electron cooler provides a monochromatic electron beam over a path length of about 2.5 m. In the electron cooling section, the fragment beam overlaps with the electron beam. In the rest frame of the cooling electrons, the fragments are similar to the particles of a hot gas. Since the electrons are continuously renewed, the ion gas evolves up to thermal equilibrium with the electron gas. As a consequence, all stored ions have an energy defined by the electrons of the cooler. This results in a reduction of their mean velocity spread.

Data aquisition

The revolution frequency of stored ion depends on their mass-to-charge ratio. By passing through two electrostatic pickup electrodes, ions induce mirror charges at each revolution. The Schottky noise signal coming from the pickup is first amplified and then digitized. Next, the amplified time signal can be recorded simultaneously on hard disks. If a Fast Fourier Transform (FFT) is applied to the time domain data, the frequency spectra obtained exhibit peak structures corresponding to specific ions. The 30th and 31st harmonics of the signal were used in the experiments. The area of any frequency peak corresponds to the integrated noise power and is proportional to the number of stored ions [32] corresponding to this peak, as well as to the square of their ionic charge. Sample data corresponding to an injection of H-like ^{140}Pr ions are shown in Fig. 3.3 and an example of a fit for ^{142}Pm is shown in Fig. 3.4

3.2 Comparison of theoretical results with experimental data

β^+ decay and electron capture probabilities of bare, hydrogen-like and helium-like ^{140}Pr, ^{142}Pm and ^{122}I ions have been measured in a few experiments and results were published in the papers [3, 28, 44, 71]. E.g. for the ^{142}Pm nucleus in total 120 injections were analyzed for H-like, He-like and fully stripped ions. Half-lives

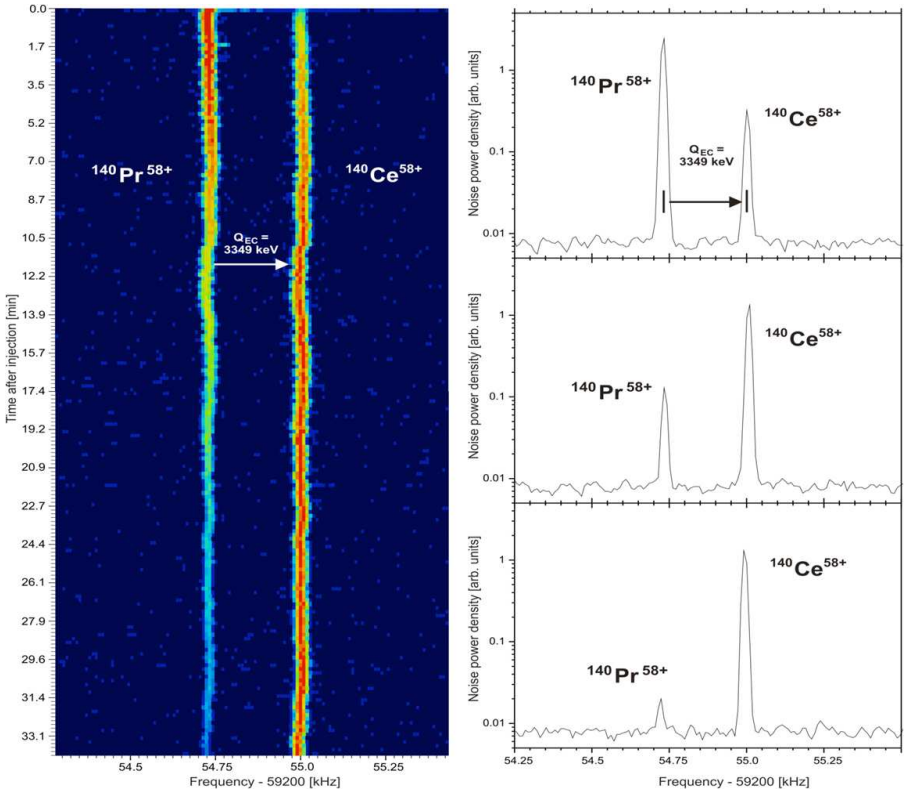

Figure 3.3: Left panel: Schottky frequency spectra at the 31st harmonic of the revolution frequency taken subsequently as a function of time (time is going from bottom to top) for hydrogen-like $^{140}Pr^{58+}$ ions. The intensity of the frequency lines is proportional to the number of stored ions. Right panel: Schottky frequency spectra at the beginning, middle and end of the measurement [70].

measured in these experiments are presented in Table 3.1. Theoretical calculations have shown that the experimental results can be explained by taking into account the conservation of the total angular momentum (and its projection) of an ion (nucleus plus leptons) [34, 52]. Using formula 2.18 and the formula derived by Z. Patyk [52], the theoretical ratio of the electron capture probabilities for He- and H-like ions can be compared with those measured in experiments.
In Table 3.2 the predicted and measured probability ratios are presented. It is clearly seen that they are consistent within experimental uncertainties. In the case of heavy ions the corrections contribute negligibly to the final ratio.

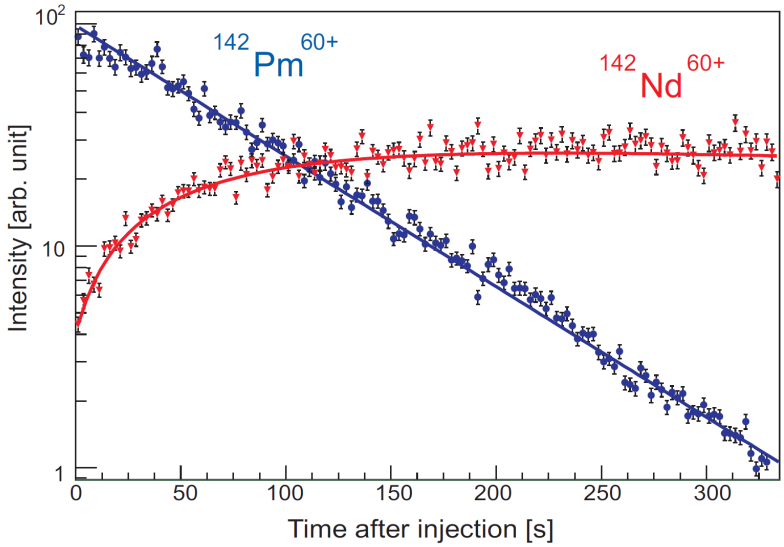

Figure 3.4: Decay and growth curves of mother $^{142}Pm^{60+}$ (in red) and daughter $^{142}Nd^{60+}$ (in blue) ions as a function of time [70].

Ion	hydrogen-like [s^{-1}]	helium-like [s^{-1}]
^{140}Pr	0.00219(5)	0.00147(7)
^{122}I	0.000735(33)	-
^{142}Pm	0.00514(14)	0.00357(10)

Table 3.1: Measured decay constants (in 1/s) for ^{140}Pr [45] and ^{142}Pm [72] ions and ^{122}I [2].

Ion	Experimental ratio	Theoretical probabilities ratio without corrections	Theoretical probabilities ratio with corrections
^{140}Pr	0.671(50)	0.667	0.661
^{142}Pm	0.681(33)		

Table 3.2: Ratios of electron capture probabilities for He- and H-like ions for nuclear transitions $1 \longrightarrow 0$. Experimental data are taken from [45] and [72] for ^{140}Pr and ^{142}Pm ions, respectively. The theoretical ratios with and without screening corrections are listed for comparison.

Chapter 4

Ionization of hydrogen-like ion in beta decay

Electron shake-off is a process in which the orbital electron is excited into the continuum as a result of a sudden change of the central potential in β decay. The ionization probability of a H-like ion in β decay is calculated in the sudden approximation limit [39, 49]. The first measurement of a pure electron shake-off following nuclear β decay, not affected by multi-electron processes such as Auger cascades, is also discussed. In this ideal textbook case for the application of the sudden approximation, the experimental ionization probability was found to be in perfect agreement with the presented quantum mechanical calculations [9].

4.1 Probability of ionization

It is assumed that the β electron is emitted with the speed of light and is distributed on a thin spherical shell of radius $R = ct$ (see Fig. 4.1). Therefore, the perturbation potential has been proposed to have the form of a constant value inside the shell:

$$\delta V(r,t) = \frac{e^2}{R}, r \leqslant ct, \tag{4.1}$$

and a Coulomb shape outside the shell

$$\delta V(r,t) = \frac{e^2}{r}, r > ct. \tag{4.2}$$

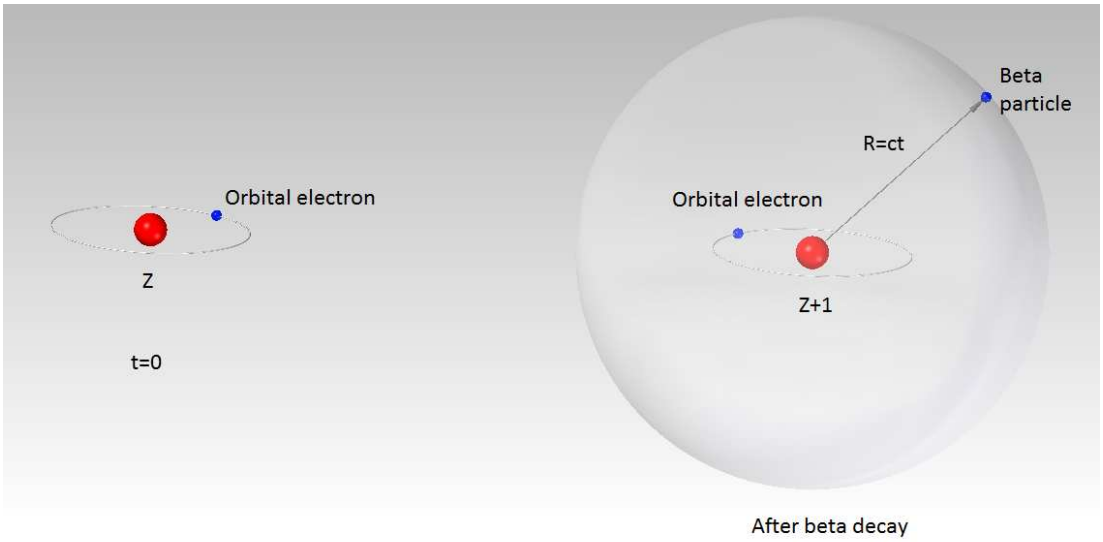

Figure 4.1: Schematic of the situation, after $t = 0$ the electron is distributed on the thin spherical shell.

The Hamiltonian for the orbital electron in a H-like ion during the beta decay process may be approximated in the following form:

$$\hat{H} = -\frac{\hbar}{2m}\nabla^2 - \frac{Z+1}{r}e^2 + \delta V(r,t). \tag{4.3}$$

The potential at t=0 equals $-\frac{Z}{r}e^2$ and after beta decay, for t$\rightarrow \infty$, the potential converges to $-\frac{Z+1}{r}e^2$.
The perturbation term multiplied by an interaction time $\langle \delta V(r,t)\delta t/\hbar \rangle$ is estimated in the following way. The perturbation term is of the order of Ze^2/a_0 and the interaction time between the beta and the orbital electrons is of the order of a_0/Zc, where a_0 denotes the Bohr radius. Combining together both findings:
$\langle \delta V(r,t)\delta t/\hbar \rangle \approx 1/137$.
The wave function $\Psi(r,t)$ of the orbital electron is expanded in the basis of eigen states of the non-perturbed Hamiltonian

$$\Psi(r,t) = \sum_n a_n(t)\psi_n(r)e^{\frac{-iE_nt}{\hbar}}. \tag{4.4}$$

Then from the Schrödinger equation

$$i\hbar\dot{\Psi}(r,t) = \hat{H}\Psi(r,t), \tag{4.5}$$

is obtained the set of equations:

$$i\hbar\sum_n \dot{a_n}(t)\psi_n(r)e^{\frac{-iE_nt}{\hbar}} = \sum_n a_n(t)\delta V(r,t)\psi_n(r)e^{\frac{-iE_nt}{\hbar}}. \tag{4.6}$$

Energies E_n are quantities of the order of Z^2e^2/a_0. However, the characteristic time for beta decay is of the order of $\delta t = a_0/Zc$ and the product $E_n\delta t \approx Z/137$. This is the reason that the energies E_n in the exponent function can be neglected for light nuclei. Assuming that the wave functions are orthogonal the relation:

$$\begin{aligned} \dot{a_m}(t) &\approx \sum_n a_n(0)\frac{1}{i\hbar}\langle m|\delta V(r,t)|n\rangle \\ &\approx \sum_n \frac{1}{i\hbar}\langle m|\delta V(r,t)|n\rangle\langle n|1s\rangle = \frac{1}{i\hbar}\langle m|\delta V(r,t)|1s\rangle \end{aligned} \tag{4.7}$$

is obtained. Solving the differential equation:

$$a_m(\delta t) = a_m(0) + \int_0^{\delta t}\frac{1}{i\hbar}\langle 1s|\delta V(r,t)|m\rangle dt, \tag{4.8}$$

where the first term is real and the second is pure imaginary, the transition probability can be expressed in the form:

$$\begin{aligned} P_{bound} &= \sum_m |a_m(\delta t)|^2 \\ &= \sum_m a_m(0)^2 + \frac{1}{\hbar^2}\sum_m(\int_0^{\delta t}\langle 1s|\delta V(r,t)|m\rangle dt)^2. \end{aligned} \tag{4.9}$$

Finally, an expression for the ionization probability:

$$P_{ionization} = 1 - \sum_m a_m(0)^2 - \frac{1}{\hbar^2}\sum_m(\int_0^{\delta t}\langle 1s|\delta V(r,t)|m\rangle dt)^2. \tag{4.10}$$

The last term can be rewritten in the form:

$$\begin{aligned} & \frac{1}{\hbar^2}\sum_m (\int_0^{\delta t}\langle 1s|\delta V(r,t)|m\rangle dt)^2 \qquad (4.11)\\ = \quad & \frac{1}{\hbar^2}\sum_m \int_0^{\delta t}\int_0^{\delta t}\langle 1s|\delta V(r,t_1)|m\rangle\langle m|\delta V(r,t_2)|1s\rangle dt_1 dt_2 \\ \cong \quad & \frac{1}{c^2\hbar^2}\int_0^{R_0}\int_0^{R_0}\langle 1s|\delta V(r,R_1)\delta V(r,R_2)|1s\rangle dR_1 dR_2, \end{aligned}$$

where the variables have been changed $dt_1 = \frac{dR_1}{c}$, $dt_2 = \frac{dR_2}{c}$. Assuming $R_1 < R_2$, integration can be done in three steps where the perturbation potential takes the form:

1. $\delta V(r,R_1)\delta V(r,R_2) = \frac{e^4}{R_1 R_2}$ when $0 < r < R_1$,
2. $\delta V(r,R_1)\delta V(r,R_2) = \frac{e^4}{r R_2}$ when $R_1 < r < R_2$,
3. $\delta V(r,R_1)\delta V(r,R_2) = \frac{e^4}{r^2}$ when $R_2 < r$.

Finally, the correction to the shake off probability [9] in a compact form:

$$\delta P_{ionization} = -\frac{1}{(\hbar c)^2}\int_0^{R_0} dR_1 \int_0^{R_0} dR_2 \langle 1s, Z|\delta V(r,R_1)\delta V(r,R_2)|1s, Z\rangle. \quad (4.12)$$

Note that the integral in the case of non limited R_0 is divergent. Therefore, the integration has to be cut for $R_0 = 2\langle 1s, Z|r|1s, Z\rangle$. Only 7% of the electron charge is distributed outside a sphere of radius R_0. The integral for $Z = 2$ has been performed numerically and the correction obtained to be equal $-20 \cdot 10^{-5}$. To calculate the ionization probability non-relativistic electron wave functions are used. In the initial state, (in atomic units) the wave function has the form:

$$|1s, Z\rangle = 2Z^{\frac{2}{3}} e^{-Zr}, \qquad (4.13)$$

where Z denotes the atomic number of the mother nucleus. However, the final state of the electron should be transformed into the laboratory frame

$$|m', Z+1\rangle = e^{-\imath \vec{k}\vec{r}}|m, Z+1\rangle, \qquad (4.14)$$

where $\vec{k}$ is the electron momentum.
The ionization probability that the orbital electron will be emitted to the continuum equals (see Eq. 4.10):

$$P_{ionization} = 1 - \sum_m a_m(0)^2 = 1 - \sum_m |\langle 1s, Z|1 - \imath\vec{k}\vec{r} - \frac{(\vec{k}\vec{r})^2}{2}|m, Z+1\rangle|^2. \quad (4.15)$$

where the exponent function was expanded up to terms in k^2. In that approximation the matrix elements have non-zero values only between states s and s or p. Higher multipolarities are excluded because they contribute with terms proportional to k^4 or higher.
There are two terms contributing to equation 4.15. The first one comes from the matrix elements between two spherical ns bound states,

$$\begin{aligned}&\langle 1s, Z|1 - \frac{(\vec{k}\vec{r})^2}{2}|ns, Z+1\rangle^2 \approx \langle 1s, Z|1|ns, Z+1\rangle^2 \\ &-\frac{(a_0k)^2}{3}\langle 1s, Z|r^2|ns, Z+1\rangle\langle 1s, Z|1|ns, Z+1\rangle, \end{aligned} \quad (4.16)$$

where all were averaged over angles $< Cos(\Theta)^2 >= 1/3$. In the second term, the matrix elements between ns and np are calculated:

$$|\langle 1s, Z| - \imath\vec{k}\vec{r}|np, Z+1\rangle|^2 = \frac{(a_0k)^2}{3}|\langle 1s, Z|r|\widetilde{np}, Z+1\rangle|^2, \quad (4.17)$$

where $\widetilde{np}$ denotes the normalized np state dependent only on the distance r. The matrix elements were calculated analytically. Finally, the ionization probability that the orbital electron escapes to the continuum after beta decay has the form:

$$\begin{aligned}&P_{ionization} = 1 - \sum_n \langle 1s, Z|1|ns, Z+1\rangle^2 \\ &+\frac{(a_0k)^2}{3}\sum_n \{\langle 1s, Z|r^2|ns, Z+1\rangle\langle 1s, Z|1|ns, Z+1\rangle \\ &-\langle 1s, Z|r|\widetilde{np}, Z+1\rangle^2\}, \end{aligned} \quad (4.18)$$

where the sum is over all bound states (ns and np). For a nucleus with six nucleons the term $(a_0 k)^2$, containing the electron momentum k

$$(a_0 k)^2 = 6.704308 * 10^{-3} [E_{recoil}/keV], \tag{4.19}$$

is transformed into an expression with the total recoil energy of the daughter nucleus.

The numerical value of the ionization probability calculated for beta decay of

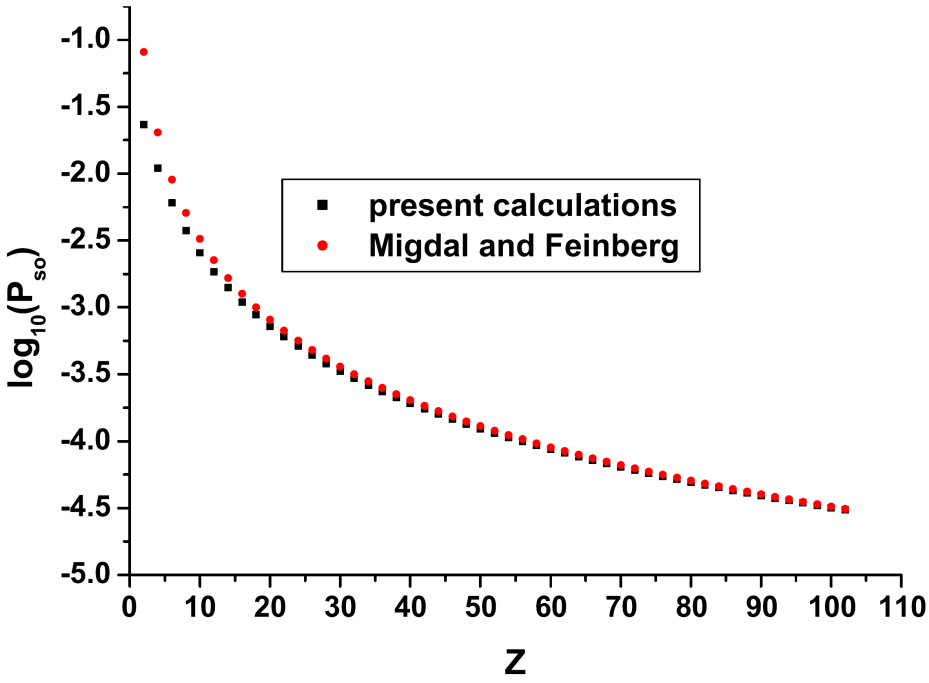

Figure 4.2: Decimal logarithm of the shake-off probability in H-like ions calculated according to Eq. 4.18 with $E_{recoil} = 0$ in comparison to the Migdal and Feinberg formula 4.21 [39] as a function of atomic number Z.

^6He equals:

$$P_{ionization} \approx 0.0233810 + 0.411874 \cdot 10^{-4} E_{recoil}[keV], \tag{4.20}$$

where E_{recoil} is the recoil energy of the daughter nucleus ^6Li. In calculations 10 000 non-relativistic H-like functions have been applied. The numerical accuracy obtained is less then 10^{-8}.
The first theoretical calculations of nuclear β decay were performed in the early 1940's by Feinberg and Migdal [48] using hydrogen like wave functions. They found for a nucleus of ^{6}He [15] the value $P_{ionization} = 0.01983$. Additionally they found the approximate formula:

$$P_{ionization} = \frac{0.325}{Z^2}. \tag{4.21}$$

In Fig. 4.2 calculated values obtained in this thesis and by Feinberg and Migdal are plotted. It is clearly seen that in the range of light nuclei ($Z < 10$) there is a discrepancy between the present calculations and the formula given by Eq. 4.21. Quite recently Wauters and Vaeck have found the ionization probability $P_{ionization} \approx 0.023$ [69].

4.2 Comparison with experiment

The electron shake-off probability of H-like $^6He^+$ ions in β^- decay was measured for the first time using a specially designed recoil ion spectrometer. Since there is only one orbital electron, the electron-electron correlation and secondary relaxation process disappear. Only two contributions to the ionization process are left. First, and dominant, is electron shake-off, caused by the rapid change of nuclear charge and the sudden recoil of the nucleus induced by the decay process. In the case of this particular ion the recoil energy can reach 1.4 keV [8]. Secondly, one possible source of ionization is a direct collision, when the β electron knocks out a bound electron. An experiment was conducted at GANIL, using the Paul trap [9, 17, 18, 57]. The radioactive ^{6}He nuclei are produced at the GANIL-SPIRAL target-ECR ion source. After mass separation by a dipole magnet, $^6He^+$ ions are guided at 10 keV through the LIRAT low energy beam line up to the entrance of the LPCTrap apparatus. At this point of the setup, a typical intensity of 1×10^8 ions of interest has been measured. The first stage of the apparatus is a Radio Frequency Cooler and Buncher (RFQCB) dedicated to beam preparation [10]. The

$^6He^+$ ions from LIRAT were injected into the RFQCB and accumulated close to the exit. The cooled ion bunches were then extracted at a repetition rate of 5 Hz and re-accelerated towards the Paul trap. The ions are transported between the two traps with a kinetic energy of about 1 keV and are decelerated down to 100 eV by a second pulsed cavity located at the entrance of the measurement trap. The Paul trap, made of six stainless steel rings is shown in Fig.4.4. The ions were confined by an RF voltage of 120 V_{pp} at 1.15 MHz continuously applied to the two inner rings whereas the intermediate rings were set to the ground potential. During the experiment, up to 2×10^4 $^6He^+$ ions were successfully trapped in the Paul trap for each 200 ms injection cycle, which corresponds to an overall transport and trapping efficiency of 1×10^{-3}. After 150 ms trapping time, the ions were extracted towards a micro-channel plate position sensitive detector (MCPPSD) dedicated to ion cloud monitoring [57] Fig. 4.3. A 4×10^{-6} mbar low

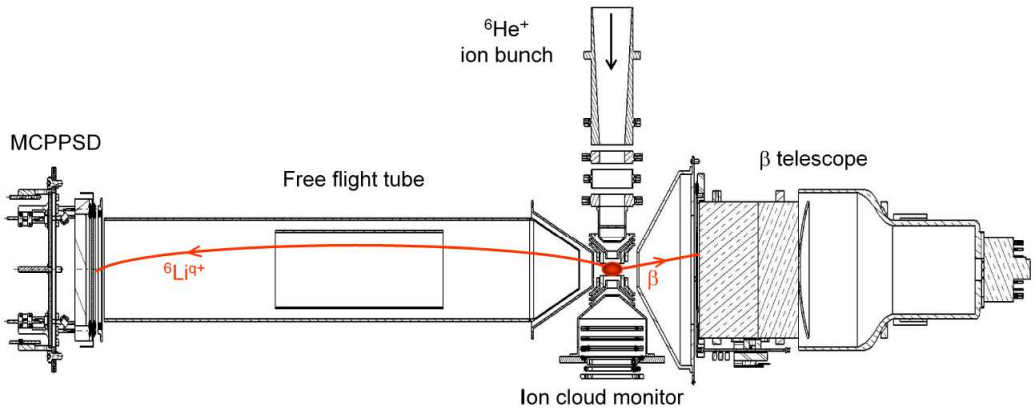

Figure 4.3: Top view of the detection chamber with the Paul trap, beta-electron telescope, the recoil ion detector and ion cloud monitor [9].

pressure H_2 buffer gas is also maintained in the trapping chamber to further cool down the trapped ions. After about 25 ms the trapped ion cloud has reached thermal equilibrium with a final thermal energy $kT \sim 0.1$ eV [19]. As shown in Fig. 4.4, β electrons and recoiling ions were detected in coincidence using two different detectors. The β telescope, made of a thin double-sided silicon strip detector (DSSSD) followed by a plastic scintillator, provides the position and the energy of the incoming beta particles. The signal from the plastic scintillator also

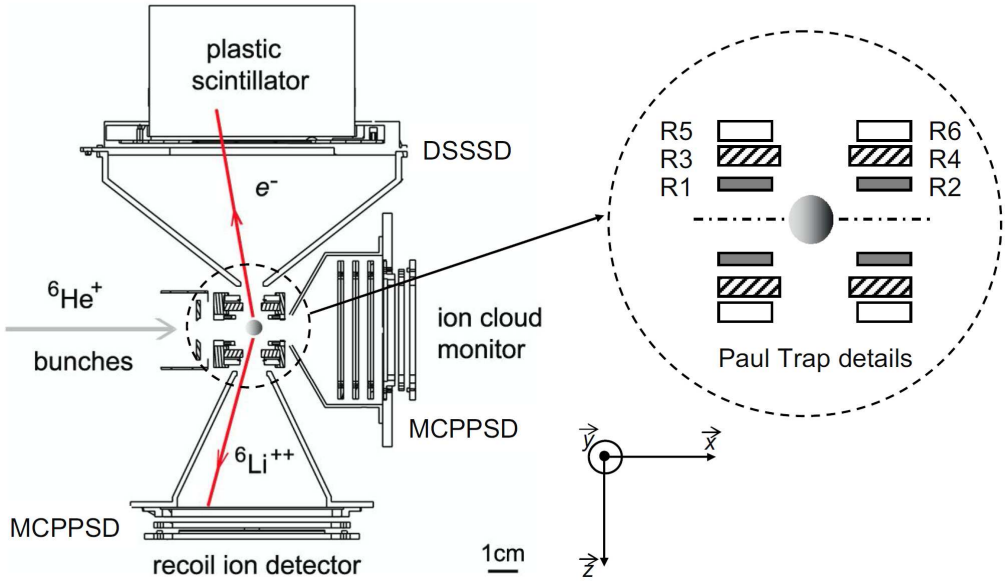

Figure 4.4: The detection chamber with the Paul trap, with an enlarged view of the Paul trap in the zoom.

triggers the acquisition system and gives the reference time of a decay event. For the detection of the daughter nuclei, a new recoil ion spectrometer was designed to measure the charge state of the recoiling ions. Those ions emitted in the adequate solid angle enter a first collimator through a 90% transmission grid set to the ground potential. They were then accelerated by a -2 kV potential applied to a second 90% transmission grid mounted on the entrance aperture of the free flight tube. Inside, an electrostatic lens at -250 V allows 100% of the ions to be collected on the recoil ion MCPPSD [40]. The acceleration voltage of -2 kV provided to the recoil ions combined with the 50 cm long free flight region allows a good separation of the time of flight (TOF) distributions obtained for $^{6}Li^{2+}$ and $^{6}Li^{3+}$ ions. For each detected event, the energy and position of the β particle, the TOF and position of the recoil ion, the time within the trapping cycle, and the RF phase of the Paul trap are recorded.

The data analysis is based on the comparison between the experimental TOF spectrum and those obtained for two sets of realistic Monte Carlo (MC) simu-

lations with, on one hand, $^6Li^{2+}$ recoil ions, and on the other hand, $^6Li^{3+}$ recoil ions resulting from electron shake-off of the daughter nuclei. For both sets, the β decay dynamics was accurately simulated using the $\beta - \nu$ angular correlation coefficient $a_{\beta\nu}$ predicted by the Standard Model, and including radiative correction terms [29]. The best fit to the electron shake-off probability is [9]: $P_{ionization} = 0.02348(35)_{stat}(06)_{syst}$. As can be seen the theoretical probability of $0.02343 - 0.00020$ is in perfect agreement with the experimentally measured value.

Chapter 5

Neutral weak interactions

Neutral weak forces are mediated by the Z boson interacting between nucleons and electrons in an atom without change of charge. The interaction does not conserve parity and can mix electron states with different parity. However, the mixing parameter is very small and depends on two factors: the amount of overlap of the electron wave function with the nucleus and the energy difference between two adjacent states of opposite parity. In this chapter an experiment is proposed in which the parity non-conservation effect could be studied in the 2^1S_0 excited state of a helium-like ion. The relative probability of nuclear electron capture in a lithium-like ion leading to the 2^1S_0 excited state in a helium-like ion was derived in Chapter 2.

5.1 PNC effect

The parity non-conservation effect in atoms and ions appears because of mixing of electronic wave functions with opposite parity. This mixing leads to an admixture of a negative-parity state ψ_- to a positive-parity state ψ_+, creating the state $\psi_+ + \eta\psi_-$. The Hamiltonian H_W determines the mixing parameter η in the first-order perturbation:

$$\eta = \frac{\langle\psi_-|H_W|\psi_+\rangle}{E_+ - E_-}, \tag{5.1}$$

where E_+ and E_- are the energies of states with even and odd parity, respectively. The spin-independent part of the effective nuclear weak-interaction Hamiltonian

is given by [60]:

$$H_W = -\frac{G_F}{2\sqrt{2}} Q_W \rho_N(r) \gamma_5, \tag{5.2}$$

where G_F denotes the Fermi constant, $Q_W \approx -N + Z(1 - 4\sin^2\theta_W)$ is the weak charge of the nucleus with N neutrons and Z protons related to the Weinberg angle θ_W, γ_5 is a Dirac matrix and ρ_N is the effective nuclear density normalized to unity.

The parity non-conservation effect in atoms is a very important probe of weak neutral interactions between electrons and nucleons. There is a possibility of using high Z He-like ions, for which precise calculations of the mixing parameter are possible. Two states 2^1S_0 and 2^3P_0 with different parity and mixed by the

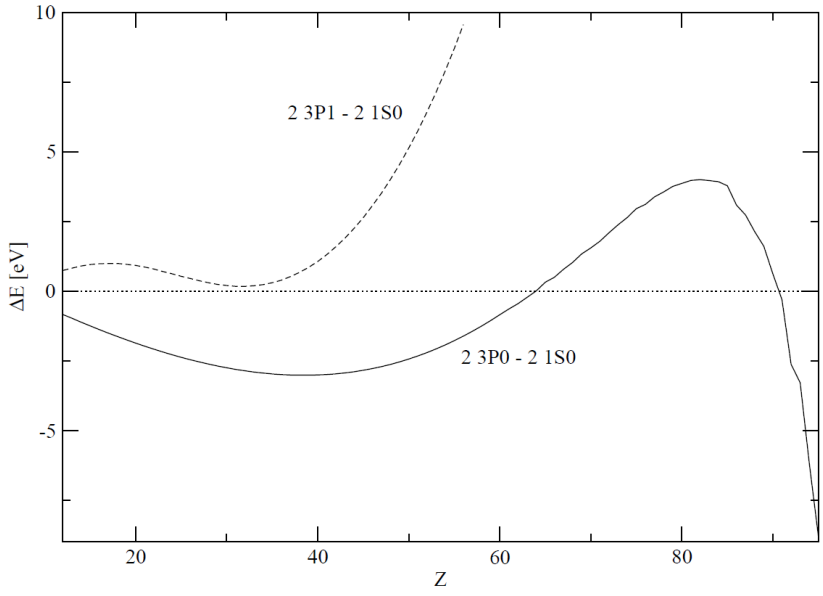

Figure 5.1: Dependance of energy splitting $2^3P_1 - 2^1S_0$ and $2^1S_0 - 2^3P_0$ in He-like ions [2] as a function of atomic number Z.

weak interaction are proposed to study the parity non-conservation effect. From Fig. 5.1 the region of atomic number Z where opposite-parity levels are in the close contact or are even degenerate can be roughly estimated. Energy levels for 2^1S_0 and 2^3P_0 states cross near atomic numbers $Z \sim 62$ and $Z \sim 90$.

In Chapter 2, the relative population probability for the 2^1S_0 state in a helium-like ion during nuclear electron capture of a lithium-like ion is derived. As can be seen in Table 2.2 the most effective way to populate the 2^1S_0 state in a helium-like ion is the nuclear transition $1 \rightarrow 0$. Based on this fact, an experiment to measure the parity non-conservation effect and a value of the mixing parameter η may be proposed.

5.2 PNC in He-like ions

The separation energy $E_{2^1S_0} - E_{2^3P_0}$ between two states has a minimum value in the vicinity of nuclei with $Z \approx 62$ or $Z \approx 90$ [2, 11, 47]. The nuclear electron capture process responsible for the formation of the $2^1S_0'$ excited state occurs around $Z \approx 62$ in the light isotopes of Pr, Nd, Pm, Sm, Eu or Gd. For heavy nuclei good candidates could be a nucleus decaying by electron capture in the vicinity of Uranium. As an example we will use a U^{90+} ion (e.g. ^{229}U or ^{231}U), illustrated in Fig 5.2.

There is a meta-stable 2^3P_0 state (with lifetime 56 ps) distant about $1\ eV$ from the 2^1S_0 state. This splitting energy is remarkably small, even compared to the $2s_{1/2} \rightarrow 2p_{1/2}$ Lamb shift in H-like Uranium, which is about 75 eV. As can be seen in Fig 5.2, the 2^1S_0 state decays exclusively by two-photon decay to the 1^1S_0 ground state. An experiment can be designed in a way to measure separately the decay rate for circular polarization of emitted photons, so that the mixing parameter η can be estimated. The polarization and the wave vector of one of the two photons can be determined and averaged over all directions and polarizations of the second one.

To account for the weak interaction the wave function of the 2^1S_0 state should first be modified due to the admixture of the 2^3P_0 state. The neutral weak interaction mixes these two states, both with zero angular momentum and different parity, so the resulting "true" eigenstate $2^1S_0'$ has the form [1]:

$$|2^1S_0'\rangle \rightarrow |2^1S_0\rangle + \frac{\langle 2^3P_0|H_W(1) + H_W(2)|2^1S_0\rangle}{E_{2^1S_0} - E_{2^3P_0}}|2^3P_0\rangle, \tag{5.3}$$

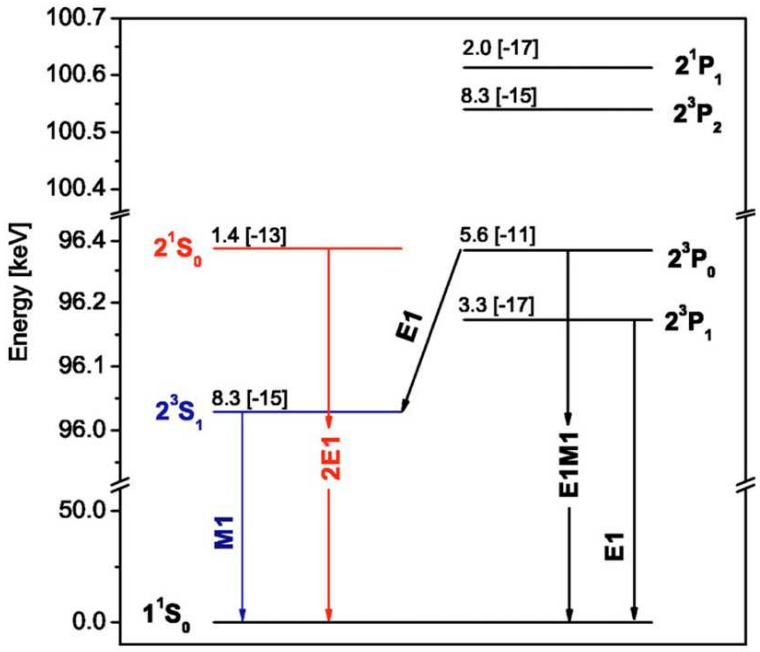

Figure 5.2: Low-lying energy levels of He-like U^{90+}, including lifetimes [s]. The numbers in brackets indicate powers of 10 [58].

where the indexes i attached to the Hamiltonian $H_W(i)$ denote an electron in a helium-like ion. The mixture parameter has the form [1, 23]:

$$\begin{aligned} \eta &= \frac{\langle 2^3P_0|H_W(1)+H_W(2)|2^1S_0\rangle}{E_{2^1S_0}-E_{2^3P_0}} \\ &= \frac{\frac{G_F}{2\sqrt{2}}Q_W\int_0^\infty drr^2\rho_N(r)[g_{2p_{1/2}}f_{2s}-f_{2p_{1/2}}g_{2s}]}{E_{2^1S_0}-E_{2^3P_0}}. \end{aligned} \tag{5.4}$$

To analyze two-photon decay, one should start with the differential decay probability

$$\frac{dw_{2\gamma}^{2^1S_0}}{d\omega_1} = \frac{\omega_1\omega_2}{(2\pi)^3c^2}|M_{2\gamma}^{2^1S_0}|^2 d\Omega_1 d\Omega_2, \tag{5.5}$$

where the ω_j are the frequencies and $d\Omega_j$ the solid angle for the j-th photon. If the summation is performed over magnetic quantum numbers the matrix element

in Eq. 5.5 has the form [13, 30]:

$$M_{2\gamma}^{2^1S_0} = -i\alpha\hat{\varepsilon}_1\hat{\varepsilon}_2 + \beta_1\hat{\varepsilon}_1(\hat{k}_2 \times \hat{\varepsilon}_2) + \beta_2\hat{\varepsilon}_2(\hat{k}_1 \times \hat{\varepsilon}_1). \tag{5.6}$$

The first term comes from the weak interaction induced $2E1$ amplitude, and the last two give the amplitude from $E1M1$ decay. The quantities $\hat{\varepsilon_j}$ and $\hat{k}_j$ denote the polarization vector and the propagation direction of the j-th photon, respectively. The coefficients have the form [13, 30, 59]:

$$\alpha = \sum_n [\frac{\langle 1^1S_0|R_{E_1}(\omega_2)|n\rangle\langle n|R_{E_1}(\omega_1)|2^1S_0\rangle}{E_n - E_{2^1S_0} + \omega_1} + \frac{\langle 1^1S_0|R_{E_1}(\omega_1)|n\rangle\langle n|R_{E_1}(\omega_2)|2^1S_0\rangle}{E_n - E_{2^1S_0} + \omega_2}],$$

$$\beta_1 = -\eta \sum_n [\frac{\langle 1^1S_0|R_{M_1}(\omega_2)|n\rangle\langle n|R_{E_1}(\omega_1)|2^3P_0\rangle}{E_n - E_{2^3P_0} + \omega_1} + \frac{\langle 1^1S_0|R_{E_1}(\omega_1)|n\rangle\langle n|R_{M_1}(\omega_2)|2^3P_0\rangle}{E_n - E_{2^3P_0} + \omega_2}],$$

$$\beta_2 = \beta_1(\omega_1 \leftrightarrow \omega_2).$$

The summation includes discrete and continuum states and $R_{M_1}(\omega_j)$ and $R_{E_1}(\omega_j)$ are $M1$ and $E1$ operators for the j-th photon. To consider possible parity experiments one can measure direction, energy and polarization of both photons. Then the decay probabilities given by Eqs. 5.5 and 5.6 are summed over the polarization and photon direction, determined for the photon denoted by the index 2. The decay probability for the photon denoted by the index 1 is expressed by the formula:

$$\frac{dw_{2\gamma}}{dk_1} = A + \eta B\hat{k}_1 \cdot \hat{\varepsilon}_1^* \times \hat{\varepsilon}_1.. \tag{5.7}$$

with two independent parameters A and ηB. However, the coefficients A and B have been calculated and can be found in the paper [13]. As a result the parameter η could be experimentally determined.
Thanks to recent technical advances in experimental techniques and position-sensitive detectors, measurements of two-photon angular correlations (investigation of the angular and polarization properties of the radiation emitted in atomic decays) could be performed within the near future e.g. at GSI-Darmstadt [59, 65, 66], which can test quantum correlations of the photon pair [24] and PNC in He-like ions [25].

Chapter 6

Conclusions

Here we collect and summarize the formulas derived and considerations raised in this thesis.

1. **Electron capture in hydrogen- and helium-like ions**

   Using Fermi's Golden rule and the wave functions derived in Chapter 2, we obtained the ratio between the decay probabilities for helium- and hydrogen-like ions.

   For the transitions $I \to I+1$

$$\begin{aligned} P_{He} = \quad & \frac{2(I \pm \frac{1}{2})+1}{2I+1} P_H \\ & \times (1 - \delta_1 + \frac{\delta_2}{Q_{EC}})(1 - \frac{5}{16Z})^3 (1 + \delta_3), \end{aligned}$$

   where $\pm$ corresponds to the nuclear transitions $I \to I+1$ and $I \to I-1$, respectively.

   For the transitions $I \to I$

$$\begin{aligned} P_{He} = \quad & (\frac{2(I+\frac{1}{2})+1}{2I+1} P_H^+ + \frac{2(I-\frac{1}{2})+1}{2I+1} P_H^-) \\ & \times (1 - \delta_1 + \frac{\delta_2}{Q_{EC}})(1 - \frac{5}{16Z})^3 (1 + \delta_3), \end{aligned}$$

   where $P_H^{\pm}$ is the probability of the EC decay in a H-like ion for the

transitions $I \pm \frac{1}{2} \rightarrow I \pm \frac{1}{2}$.

It turns out that the most significant contribution of all the corrections obtained is the electron screening effect. The correction has a simple form $(1 - 5/16Z)^3(1 - \delta_3)$ which ranges from almost fifty percent in helium to one percent in heavier nuclei.

2. **Electron capture for He-like and H-like ions in a hot environment.** Electron capture in ^{7}Be has astrophysical consequences. In a hot environment, where the temperature is higher than the hyperfine splitting energy, states in a H-like ion are populated statistically. The calculated ratio of probabilities in electron capture of He-like and H-like ions equals 1.57. However, without the screening corrections the ratio equals 2.

3. **Ionization probability in electron capture of a helium-like ion.**

   A new electron capture decay channel in a helium-like ion with emission of orbital electron into the continuum was briefly discussed. The estimated ionization probability reaches a value of about 10% for light nuclei and monotonically decreases down to 5.6×10^{-5} for Pb isotopes.

4. **Population of excited states in a helium-like ion**

   From ratios derived in Chapter 2, one can find that a daughter helium-like ion is created mostly in the 2^1S_0 and 2^3P_1 excited states. The ratio of population probabilities for these two states depends on the spin I of the mother nucleus and the type of the electron capture transition:

$$\frac{P_{2^1S_0}}{P_{2^3P_1}} = \frac{2I+1}{2(I \pm 1)+1}.$$

5. **Electron capture in a lithium-like ion**

   Additionally, the following simple relation between the probabilities of electron capture for lithium- and hydrogen-like ions has been found:

$$P_{Li} = P_H\left(\frac{2(I \pm 1/2)+1}{(2I+1)} + \frac{\rho^{2s}(Z)}{2\rho^{1s}(Z)}\right)\left(1 - \frac{q}{Z}\right)^3,$$

where q=0.464.

6. **Ionization probability in beta decay**

   Using the sudden approximation the ionization probability of an orbital electron during the beta decay process in a H-like ^{6}He ion has been derived. The probability obtained is in a perfect agreement with measurement.

7. **Neutral weak interaction**

   As an example, the parity non-conservation effect in a helium-like ion was briefly discussed. The $2^1S_0'$ excited state is a linear combination of the 2^1S_0 and 2^3P_1 states, both with zero angular momentum and different parity. A method how to determine the a mixing parameter from the two-photon transition to the ground state was proposed.

8. **Experimental applications**

   There are several areas where the formulas obtained in this thesis could be applied.

   First is the possibility of spin measurement in the mother nucleus of a decaying ion. This is especially important for short lived neutron-deficient exotic nuclei, which mostly have unknown ground state spin values. Assuming the type of the orbital EC transition in lithium-like ion ($I \to I \pm 1$) and measuring the ratio $P_{2^1S_0}/P_{2^3P_1}$, the spin I in the mother nucleus can be experimentally determined from Eq. 2.36.

   As a second application one could measure the ratio of relativistic 2s and 1s electron densities at the nucleus. From the experimentally determined ratio P_{Li}/P_H together with additional knowledge of the type of the orbital electron capture transition the density ratio could be determined from Eq. 2.38.

Appendix A- Dirac equation and Dirac spinors

The Dirac equation has the form [14]

$$H\Psi = [\alpha \cdot \mathbf{p}c + \beta mc^2 + V(r)]\Psi, \tag{1}$$

where $V{=}\frac{-Ze^2}{r}$ is the Coulomb potential. The spinor, for the problem of a central field can be written as:

$$\Psi = \begin{bmatrix} f(r)\varphi_{jm}^{(l)} \\ -ig(r)\frac{\sigma\cdot\mathbf{r}}{r}\varphi_{jm}^{(l)} \end{bmatrix}, \tag{2}$$

There exist two types of the two-component angular functions:

$j = l + \frac{1}{2}$

$$\varphi_{jm}^{(l)} = \begin{bmatrix} \sqrt{\frac{l+1/2+m}{2l+1}}Y_l^{m-1/2} \\ \sqrt{\frac{l+1/2-m}{2l+1}}Y_l^{m+1/2} \end{bmatrix}, \tag{3}$$

$j = l - \frac{1}{2}$

$$\varphi_{jm}^{(l)} = \begin{bmatrix} \sqrt{\frac{l+1/2-m}{2l+1}}Y_l^{m-1/2} \\ -\sqrt{\frac{l+1/2+m}{2l+1}}Y_l^{m+1/2} \end{bmatrix}, \tag{4}$$

where the latter function exists only for $l > 0$. Spherical harmonics satisfy the following condition: $Y_{l,m}^* = (-1)^m Y_{l,-m}$. Both component functions are also eigen-

functions of the angular momentum J^2 and its projection J_z

$$J^2\varphi_{jm}^{(l)} = j(j+1)\varphi_{jm}^{(l)}.$$

The energy spectrum of Eq. 1 is expressed in the form [14]

$$E_n = mc^2\left[1+\left(\frac{Z\alpha}{n-(j+\frac{1}{2})+\sqrt{(j+\frac{1}{2})^2-Z^2\alpha^2}}\right)^2\right]^{-\frac{1}{2}}, \tag{5}$$

where $n = 1, 2, \ldots, \infty$ and the eigenvalues of angular momentum l satisfy the condition $0 \leqslant l \leqslant n-1$.
As an example the normalized eigenfunctions corresponding to the ground state (with $n = 1$ and $j = 1/2$) are:

$$|-\rangle^{1s} = \frac{(2mZ\alpha)^{3/2}}{\sqrt{4\pi}}\sqrt{\frac{1+\gamma}{2\Gamma(1+2\gamma)}}(2mZ\alpha)^{\gamma-1}e^{mZ\alpha r}\begin{pmatrix} 0 \\ 1 \\ \frac{i(1-\gamma)}{2\alpha}\sin\theta e^{-i\phi} \\ \frac{-i(1-\gamma)}{2\alpha}\cos\theta \end{pmatrix},$$

$$|+\rangle^{1s} = \frac{(2mZ\alpha)^{3/2}}{\sqrt{4\pi}}\sqrt{\frac{1+\gamma}{2\Gamma(1+2\gamma)}}(2mZ\alpha)^{\gamma-1}e^{-mZ\alpha r}\begin{pmatrix} 1 \\ 0 \\ \frac{i(1-\gamma)}{2\alpha}\cos\theta \\ \frac{i(1-\gamma)}{2\alpha}\sin\theta e^{-i\phi} \end{pmatrix}, \tag{6}$$

where $\gamma = \sqrt{1-(Z\alpha)^2}$.

Appendix B- Relativistic screening correction

The Hamiltonian for two self-interacting electrons in the field of a nucleus with electric charge Ze has the form

$$H = [\alpha \cdot \mathbf{p_1} c + \beta mc^2] - \frac{Ze^2}{r_1} + [\alpha \cdot \mathbf{p_2} c + \beta mc^2] - \frac{Ze^2}{r_2} + \frac{e^2}{r_{12}}, \tag{7}$$

where electrons $e1$ and $e2$ are marked as shown in Fig. 1. p_i- are momentum operators for each electron [6], $\frac{Ze^2}{r_i}$- is responsible for the interaction with the nucleus, $\frac{e^2}{r_{12}}$- is partly responsible for the interaction between the electrons. In the next step the parameter: $Z' = Z - q$ is introduced, marked later as the effective charge of the nucleus, where q denotes the screening correction, then the hamiltonian has the form

$$\begin{aligned} H &= [\alpha \cdot \mathbf{p_1} c + \beta mc^2] - \frac{Z'e^2}{r_1} + [\alpha \cdot \mathbf{p_2} c + \beta mc^2] - \frac{Z'e^2}{r_2} \\ &+ \frac{(Z' - Z)'e^2}{r_2} + \frac{(Z' - Z)e^2}{r_2} + \frac{e^2}{r_{12}}. \end{aligned} \tag{8}$$

As a wave function we use a product of two hydrogen-like wave functions in the ground state, given by Eq. 6, taken with an effective nuclear charge $Z'e$. In this

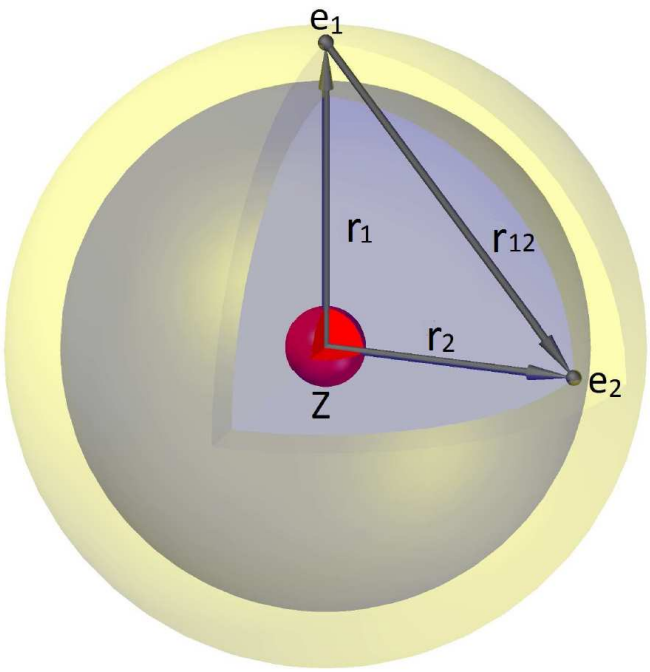

Figure 1: He-like ion with two self-interacting electrons $e1$ and $e2$ in the field of a nucleus with charge Ze

case the expected values are equal to

$$\langle \alpha \cdot \mathbf{p_1} c + \beta mc^2 - \frac{Z'e^2}{r_1} \rangle = mc^2 \sqrt{1-(\alpha Z')^2}, \tag{9}$$

$$\langle \alpha \cdot \mathbf{p_2} c + \beta mc^2 - \frac{Z'e^2}{r_2} \rangle = mc^2 \sqrt{1-(\alpha Z')^2}, \tag{10}$$

where α is fine structure constant.
The energy of the two electrons as a the function of parameters Z' and Z can be written as:

$$E(Z,Z') = 2mc^2\sqrt{1-(\alpha Z')^2} + (Z'-Z)e^2\langle\frac{1}{r_1}\rangle + (Z'-Z)e^2\langle\frac{1}{r_2}\rangle + e^2\langle\frac{1}{r_{12}}\rangle, \tag{11}$$

The second and third component are equal to:

$$\langle\frac{e^2}{r_1}\rangle = mc^2\frac{Z'}{\gamma},$$
$$\langle\frac{e^2}{r_2}\rangle = mc^2\frac{Z'}{\gamma}. \tag{12}$$

The latter component equals:

$$\langle\frac{e^2}{r_{12}}\rangle = mc^2 Z'\frac{\gamma\Gamma(2\gamma)^2 - \Gamma(4\gamma)2^{-4\gamma}}{(\gamma\Gamma(2\gamma))^2} \tag{13}$$

where $\Gamma(x)$ denotes the gamma function.
The final expression for the energy of two self-interacting electrons in the potential of a point-like nucleus with charge Ze has the form:

$$E(Z,Z') = mc^2(2\sqrt{1-(\alpha Z')^2} + 2\alpha^2\frac{Z'(Z'-Z)}{\gamma} + \alpha^2 Z'\frac{\gamma\Gamma(2\gamma)^2 - \Gamma(4\gamma)2^{-4\gamma}}{(\gamma\Gamma(2\gamma))^2}). \tag{14}$$

The latter expression should be minimized numerically with respect to $Z' = Z - q$ with fixed nuclear charge Ze. The corrections q are presented in Fig. 2.1, page 18 and Table 2.1, page 17.

Appendix C- Hyperfine splitting

A nuclei with an odd number of protons or neutrons mostly have non-zero spin value I and a nuclear magnetic dipole moment μ. A H-like ion with one electron in the 1s orbit has two electronic states with a total angular momentum equal to $F^{\pm} = I \pm \frac{1}{2}$. These two states, due to the coupling of the magnetic moments of the electron with the nucleus have slightly different energies. The state F^{-} has a lower energy than F^{+} for positive nuclear magnetic moment and vice versa. The electron energy of the hyperfine splitting δE is given by the equation:

$$\delta E = \frac{4}{3}\alpha(\alpha Z)^3 \frac{\mu}{\mu_N}\frac{m}{m_p}\frac{2I+1}{2I}A(\alpha Z)mc^2, \tag{15}$$

where m, m_p, μ, μ_N and α denote the mass of electron, the mass of proton, the nuclear magnetic moment, the nuclear magneton and the fine structure constant, respectively. The function $A(\alpha Z)$ has the form:

$$A(\alpha Z) = \frac{1}{(2\sqrt{1-(\alpha Z)^2}-1)\sqrt{1-(\alpha Z)^2}}. \tag{16}$$

The transition probability from the excited state $F^{\pm}$ to the ground state $F^{\mp}$ is given by the expression:

$$W_{F^{\pm}\to F^{\mp}} = \frac{4\alpha}{3}\delta E^3 \frac{1}{\hbar m^2 c^4}\frac{2F^{\mp}+1}{2I+1}. \tag{17}$$

In Table 1 the hyperfine splitting energies for transitions between the hyperfine states are listed. Energies vary from mili-electronvolts up to the order of several electronvolts.
In a hydrogen-like ion the electron capture transition $1 \rightarrow 0$ is allowed for an F^- state. Only beta decay can take place from the F^+ state (see Fig. 2).
This example shows that nuclear transitions in H-like ions are governed by a few

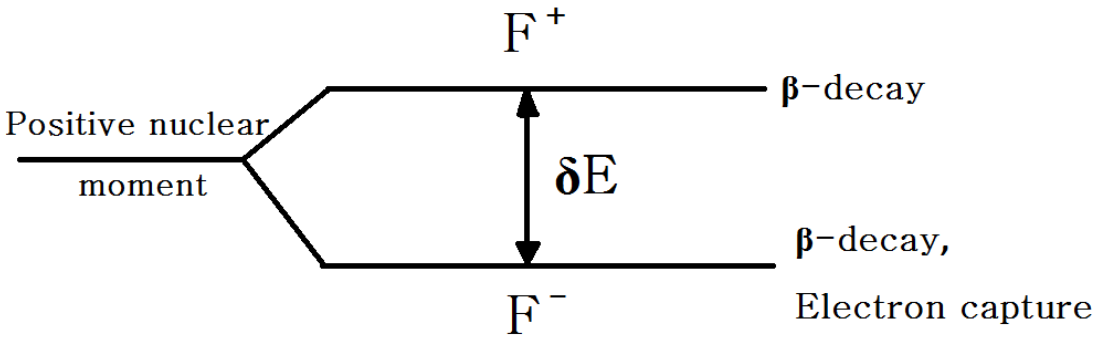

Figure 2: Possible transitions from states with $F^{\pm}$ for H-like ion with positive nuclear magnetic moment.

electronvolts hyperfine splitting.

$H-like\ ion$	$I_i^{\pi_i} \rightarrow I_f^{\pi_f}$	$\frac{\mu}{\mu_N}$	$\delta E(eV)$	$\tau_{1/2}$
^{19}Ne	$\frac{1}{2}^+ \rightarrow \frac{1}{2}^+$	-1.89	0.004	$3d$
^{37}Ar	$\frac{3}{2}^+ \rightarrow \frac{3}{2}^+$	$+1.15$	0.01	10 h
^{64}Cu	$1^+ \rightarrow 0^+$	-0.22	0.009	7h
^{68}Ga	$1^+ \rightarrow 0^+$	$+0.01$	0.001	5 yr
^{71}Ge	$\frac{1}{2}^- \rightarrow \frac{3}{2}^-$	$+0.55$	0.041	12 min
^{108}Ag	$1^+ \rightarrow 0^+$	$+2.69$	0.53	0.24 s
^{131}Cs	$\frac{5}{2}^+ \rightarrow \frac{3}{2}^+$	$+3.54$	0.98	31 ms
^{141}Nd	$\frac{3}{2}^+ \rightarrow \frac{5}{2}^+$	$+1.01$	0.43	0.4 s
^{178}Ta	$1^+ \rightarrow 0^+$	$+2.74$	2.87	16 ms

Table 1: The hyperfine splittings δE and half-lives $\tau_{1/2}$ for the transitions between hyperfine states for several H-like ions. Experimental values of magnetic moments μ are taken from [56].

References

[1] P.M.D.G. Amaro. *Study of Forbidden Transitions in Atomic Systems.* PhD thesis, FCT-UNL UPMC, 2011. 50, 51

[2] A.N. Artemyev et al. *Phys. Rev. A*, **71**:062104, 2005. 36, 49, 50

[3] D.R. Atanasov. *Eur. Phys. J. A.*, **48**:22, 2012. 34

[4] W. Bambynek et al. *Rev. Mod. Phys.*, **49**:77, 1977. 4, 6

[5] H. Becquerel. *Comptes Rendus*, **122**:420, 1986. 3

[6] J.D. Bjorken and S.D. Drell. *Relativistic quantum mechanics.* McGraw-Hill Book Company, 1964. 12, 59

[7] F. Bosch et al. *Phys. Rev. Lett.*, **77**:5190, 1996. 31

[8] T.A. Carlson et al. *Phys. Rev.*, **169**:27, 1968. 44

[9] C. Couratin et al. *Phys. Rev. Lett.*, **108**:243201, 2012. 2, 38, 41, 44, 45, 47

[10] G. Darius et al. *Rev. Sci. Instrum.*, **75**:4804, 2004. 44

[11] A. Derevianko and W.R. Johnson. *Phys. Rev. A*, **56**:1288, 1997. 50

[12] W.R. Johnson D.R. Plante and J. Sapirstein. *Phys. Rev. A*, **49**:3519, 1994. 22

[13] R.W. Dunford. *Phys. Rev. A*, **54**:3820, 1996. 52, 53

[14] L.P. Pitaevskii DV.B. Berestetskii and E.M. Lifshitz. *Quantum Electrodynamics*. Butterworth-Heinemann, Oxford, 1982. 11, 12, 57, 58

[15] E.L. Feinberg. *J. Phys. (USSR)*, **4**:423, 1941. 44

[16] R.P. Feynman and M. Gell-Mann. *Phys. Rev.*, **109**:193, 1958. 4, 14

[17] X. Fléchard et al. *Phys. Rev. Lett.*, **101**:212504, 2008. 44

[18] X. Fléchard et al. *J. Phys. G: Nucl. Part. Phys.*, **38**:055101, 2011. 44

[19] X. Fléchard et al. *Hyperfine Interact*, **199**:21, 2011. 45

[20] B. Franzke. *Nucl. Instr. and Meth. B*, **18**:24–25, 1987. 32

[21] B. Franzke et al. *Nucl. Instr. Meth.*, **B24/25**:18, 1987. 32

[22] B. Franzke et al. *Phys. Scr*, **T59**:176, 1995. 32

[23] F. Fratini. *Polarization and correlation phenomena in the two-photon absorption and decay of heavy ions*. PhD thesis, Ruperto-Carola-University of Heidelberg, 2011. 51

[24] F. Fratini et al. *Phys. Rev. A*, **83(3)**:032506, 2011. 53

[25] F. Fratini et al. *Phys. Rev. A*, **83(3)**:052505, 2011. 53

[26] H. Geissel et al. *Phys. Rev. Lett.*, **68**:3412, 1992. 31

[27] H. Geissel et al. *Nucl. Instr. and Meth. B*, **70**:286, 1992. 32

[28] H. Geissel et al. *Eur. J. Sp. Topics*, **150**:109, 2007. 1, 34

[29] F. Gluck. *Nucl. Phys. A*, **628**:493, 1998. 47

[30] S.P. Goldman and G.W.F. Drake. *Phys. Rev. A*, **24**:183, 1981. 52

[31] B. Franzke H. Geissel and G. Muenzeberg. *Experimental proposal for the SIS-FRS-ESR facilities*. 1987. 32

[32] R.W. Hasse et al. *Phys. Rev. Lett.*, **90**:204801, 2003. 34

[33] H. Inrich et al. *Phys. Rev. Lett.*, **75**:4182, 1995. 31

[34] A.N. Ivanov et al. *Phys. Rev. C*, **78**:025503, 2008. 35

[35] W.R. Johnson and G. Soff. *Atomic Data and Nuclear Data Tables*, **33**:405, 1985. 22

[36] M. Jung et al. *Phys. Rev. Lett.*, **69**:2164, 1992. 31

[37] R. Khatri and R.A. Sunyaev. *Astr. Lett.*, **37(6)**:367, 2011. 25

[38] L.N. Labzowsky et al. *Phys. Rev. A*, **63**:054105, 2001. 25

[39] L.D. Landau and E.M. Lifshitz. *Quantum Mechanics: Non-Relativistic Theory*. Butterworth-Heinemann, Oxford, 1982. 15, 18, 19, 38, 43

[40] E. Liénard et al. *Nucl. Instrum. Methods Phys. Res. A*, **551**:375, 2005. 46

[41] Yu.A. Litvinov and F. Bosch. *Rep. Prog. Phys.*, **74**:016301, 2011. 31

[42] Yu.A. Litvinov et al. *Nucl. Phys. A*, **734**:473, 2004. 31

[43] Yu.A. Litvinov et al. *Nucl. Phys. A*, **756**:3, 2005. 31, 33

[44] Yu.A. Litvinov et al. *Phys. Rev. Lett.*, **99**:262501, 2007. 1, 34

[45] Yu.A. Litvinov et al. *Phys. Lett. B*, **664**:162, 2008. 36, 37

[46] Yu.A. Litvinov et al. *Acta Phys. Polonica B*, **41**:511, 2010. 31

[47] A.V. Maiorova et al. *J. Phys. B*, **42**:205002, 2009. 50

[48] A.B. Migdal. *J. Phys. (USSR)*, **4**:449, 1941. 44

[49] A.B. Migdal. *Jakościowe metody w teorii kwantowej*. PWN, Warszawa, 1980. 38

[50] F. Nolden et al. *Nucl. Instr. and Meth.*, **A441**:219, 2000. 34

[51] T. Othsubo et al. *Phys. Rev. Lett.*, **95**:052501, 2005. 31

[52] Z. Patyk et al. *Phys. Rev. C*, **77**:014306, 2008. 1, 2, 35

[53] M. Puchalski. *Phys. Rev. A*, **80**:032521, 2009. 12

[54] T. Radon et al. *Phys. Rev. Lett.*, **78**:4701, 1997. 31

[55] T. Radon et al. *Nucl. Phys. A*, **677**:75, 2000. 31

[56] P. Raghavan. *Atomic Data and Nuclear Data Tables*, **42**:189, 1989. 64

[57] D. Rodríguez et al. *Nucl. Instrum. Methods Phys. Res. A*, **565**:876, 2006. 44, 45

[58] J. Rzadkiewicz et al. *Phys. Rev. A*, **74**:012511, 2006. 25, 51

[59] R.W. Schmieder. *Phys. Rev. A*, **7**:1458, 1973. 52, 53

[60] V.M. Shabaev et al. *Phys. Rev. A*, **81**:052102, 2010. 49

[61] K. Siegień-Iwaniuk et al. *Phys. Rev. C*, **84**:014301, 2011. 2

[62] K. Siegień-Iwaniuk and Z. Patyk. *Phys. Rev. C*, **84**:064309, 2011. 2

[63] M. Steck et al. *AIP Conf. Proc.*, **457**:87, 1999. 33

[64] M. Steck et al. *Nucl. Instr. and Meth.*, **A532**:357, 2004. 34

[65] Th. Stöohlker. *J. Phys.: Conf. Ser.*, **58(1)**:411, 2007. 53

[66] S. Tashenov et al. *Phys. Rev. Lett.*, **97(22)**:223202, 2006. 53

[67] D.R. Tilley et al. *Nucl. Phys. A*, **708**:3, 2002. 23

[68] S. Toleikis et al. *Phys. Rev. A*, **69**:022507, 2004. 25

[69] L. Wauters and N. Vaeck. *Phys. Rev. C*, **53**:497, 1996. 44

[70] N. Winckler. *Orbital electron capture of stored highly ionized* ^{140}Pr *and* ^{142}Pm *ions*. PhD thesis, Justus-Liebig Universitaet Giessen, 2008. 35, 36

[71] N. Winckler et al. *Phys. Lett. B*, **679**:36, 2009. 34

[72] N. Winckler et al. *Phys. Lett. B*, **679**:36, 2009. 36, 37

[73] J.W. Xia et al. *Nucl. Instr. and Meth. A*, **488**:11, 2002. 32

[74] G.Q. Xiao et al. *Int. J. Mod. Phys. E*, **18**:405, 2009. 32